

Supporting Information for  
**Controlled Polymerization of  $\beta$ -Pinadiene: Accessing Unusual Polymer Architectures with Biomass-Derived Monomers**  
*Alan D. Fried and Johnathan N. Brantley\**  
*Department of Chemistry, University of Tennessee, Knoxville, Tennessee 37916*  
Email: [jbrant13@utk.edu](mailto:jbrant13@utk.edu)

**Table of Contents**

|          |  |     |
|----------|--|-----|
| <b>1</b> | <b>General Considerations</b>  | S5  |
| 1.1.     | Materials and Methods  | S5  |
| <b>2</b> | <b>Monomer Synthesis</b>   | S5  |
| 2.1.     | Synthesis of <b>1</b>  | S5  |
|          | Scheme S1: Synthesis of <b>1</b>   | S5  |
| 2.2.     | Synthesis of <b>2</b>  | S6  |
|          | Scheme S2: Synthesis of <b>2</b>   | S6  |
| <b>3</b> | <b>Polymerization Studies and Material Characterization</b>                            | S6  |
| 3.1      | General Procedure for the Vinyl-Addition Polymerization of <b>2</b> using <b>4</b>     | S6  |
|          | Scheme S3: Generation of <b>4</b> <i>in situ</i> and Synthesis of <b>3</b>             | S6  |
|          | Table S1: Representative Range of Molecular Weights Accessible Using <b>4</b>          | S7  |
|          | Figure S1: Selected GPC Data for <b>3</b>  | S7  |
| 3.1.1    | Confirmation of Fused-Ring Structure of <b>3</b>                                       | S8  |
| 3.2.     | Procedure for the Vinyl-Addition Polymerization of <b>2</b> Using <b>5</b>             | S8  |
|          | Scheme S4: Vinyl-Addition Polymerization of <b>2</b> Using <b>5</b>                    | S8  |
|          | Figure S2: GPC Data for the Vinyl-Addition Polymerization of <b>2</b> Using <b>5</b>   | S9  |
| 3.3      | Procedure for the Vinyl-Addition Polymerization of <b>2</b> Using <b>6</b>             | S9  |
|          | Scheme S5: Vinyl-Addition Polymerization of <b>2</b> Using <b>6</b>                    | S9  |
|          | Figure S3: GPC Data for the Vinyl-Addition Polymerization of <b>2</b> Using <b>6</b>   | S10 |
| 3.4      | Initiator Screen for Other Polymerizations of <b>2</b>                                 | S10 |
| 3.4.1    | General Procedure for the Uncontrolled Radical Ring-Opening Polymerization of <b>2</b> | S10 |
| 3.4.2    | General Procedure for the Controlled Radical Ring-Opening Polymerization of <b>2</b>   | S10 |

|  |     |
|--|-----|
| 3.4.3 General Procedure for the Anionic Ring-Opening Polymerization of <b>2</b>              | S11 |
| 3.4.4 General Procedure for the Cationic Ring-Opening Polymerization of <b>2</b>             | S11 |
| 3.4.5 Cationic Ring-Opening Polymerization of <b>2</b> with $\text{AlCl}_3\text{OPh}_2$      | S11 |
| Scheme S6: Cationic Ring-Opening Polymerization of <b>2</b> with $\text{AlCl}_3\text{OPh}_2$ | S11 |
| Figure S4: GPC Data for the Ring-Opening Polymerization of <b>2</b>                          | S12 |
| Table S2: Initiator Screen for the Ring-Opening Polymerization of <b>2</b>                   | S12 |
| 3.5 Procedure for the Preparation of <b>7</b>  | S12 |
| Scheme S7: Preparation of <b>7</b>   | S12 |
| Figure S5: GPC Data for <b>7</b>   | S13 |
| 3.6 Thermomechanical Data  | S13 |
| 3.6.1 TGA and DMA Data for <b>3</b>  | S13 |
| Figure S6: Representative TGA Thermogram of <b>3</b>   | S14 |
| Figure S7: Representative Powder DMA of <b>3</b>   | S14 |
| 3.6.2 TGA and DMA Data for <b>7</b>  | S14 |
| Figure S8: Representative TGA Thermogram of <b>7</b>   | S15 |
| Figure S9: Representative Powder DMA of <b>7</b>   | S15 |
| 3.6.3 WAXS Measurements of <b>3</b>  | S15 |
| Figure S10: WAXS Spectrum of Low Molecular Weight <b>3</b>                                   | S16 |
| Figure S11: WAXS Spectrum of High Molecular Weight <b>3</b>                                  | S16 |
| Figure S12: WAXS Spectrum of Annealed <b>3</b>   | S17 |
| Table S3: WAXS Data for <b>3</b>   | S17 |
| 3.6.4 WAXS Measurements of <b>7</b>  | S17 |
| Figure S13: WAXS Spectrum of <b>7</b>  | S18 |
| Figure S14: WAXS Spectrum of Annealed <b>7</b>   | S18 |
| Table S4: WAXS Data for <b>7</b>   | S19 |
| <b>4 Determination of Living Character</b>   | S19 |
| 4.1 Molecular Weight as a Function of Monomer Conversion                                     | S19 |
| Table S5: Living Plot Molecular Weight and Conversion Data                                   | S19 |
| 4.2 Chain Extension Experiment   | S19 |
| Table S6: Molecular Weight Data for Chain Extension of <b>3</b>                              | S20 |
| <b>5 NMR Spectroscopic Data</b>  | S20 |

|  |     |
|--|-----|
| Figure S15: $^1\text{H}$ NMR Spectrum of <b>1</b>  | S20 |
| Figure S16: $^{13}\text{C}$ NMR Spectrum of <b>1</b>   | S21 |
| Figure S17: $^1\text{H}$ NMR Spectrum of <b>2</b>  | S21 |
| Figure S18: $^{13}\text{C}$ NMR Spectrum of <b>2</b>   | S22 |
| Figure S19: $^1\text{H}$ - $^{13}\text{C}$ HSQC NMR Spectrum of <b>2</b>   | S22 |
| Figure S20: $^1\text{H}$ - $^1\text{H}$ COSY NMR Spectrum of <b>2</b>  | S23 |
| Figure S21: $^1\text{H}$ NMR Spectrum for <b>3</b>   | S23 |
| Figure S22: $^{13}\text{C}$ NMR Spectrum for <b>3</b>  | S24 |
| Figure S23: $^1\text{H}$ - $^1\text{H}$ COSY NMR Spectrum for <b>3</b>   | S24 |
| Figure S24: $^1\text{H}$ - $^{13}\text{C}$ HSQC NMR Spectrum for <b>3</b>  | S25 |
| Figure S25: $^1\text{H}$ NMR Spectrum for the Polymerization of <b>2</b> Using <b>5</b>                            | S25 |
| Figure S26: $^1\text{H}$ NMR Spectrum for the Polymerization of <b>2</b> Using <b>6</b>                            | S26 |
| Figure S27: $^1\text{H}$ NMR Spectrum for Cationic Ring-Opening Polymerization of <b>2</b>                         | S26 |
| Figure S28: $^1\text{H}$ NMR Spectrum for <b>7</b>   | S27 |
| Figure S29: $^{13}\text{C}$ NMR Spectrum for <b>7</b>  | S27 |
| <b>6 Raw GPC Data</b>  | S28 |
| Figure S30: Raw GPC Data for Table S1 Entry 1  | S28 |
| Figure S31: Raw GPC Data for Table S1 Entry 2  | S28 |
| Figure S32: Raw GPC Data for Table S1 Entry 3  | S29 |
| Figure S33: Raw GPC Data for Table S1 Entry 4  | S29 |
| Figure S34: Raw GPC Data for Table S1 Entry 5  | S30 |
| Figure S35: Raw GPC Data for Table S1 Entry 6  | S30 |
| Figure S36: Raw GPC Data for the Vinyl-Addition Polymerization of <b>2</b> With <b>5</b>                           | S31 |
| Figure S37: Raw GPC Data for the Vinyl-Addition Polymerization of <b>2</b> With <b>6</b>                           | S31 |
| Figure S38: Raw GPC Data for the Cationic Ring-Opening Polymerization of (1S)-(-)- $\beta$ -pinene                 | S32 |
| Figure S39: Raw GPC Data for the Polymerization of <b>2</b> With <b>4</b> in Toluene (for Solvent Screen)          | S32 |
| Figure S40: Raw GPC Data for the Polymerization of <b>2</b> With <b>4</b> in Toluene at 35 °C (for Solvent Screen) | S33 |

|   |     |
|---|-----|
| Figure S41: Raw GPC Data for the Polymerization of <b>2</b> With <b>4</b> in Et <sub>2</sub> O (for Solvent Screen) | S33 |
| Figure S42: Raw GPC Data for the Polymerization of <b>2</b> With <b>4</b> in THF (for Solvent Screen)               | S34 |
| Figure S43: Raw GPC Data for the Polymerization of <b>2</b> With <b>4</b> in DCM (for Solvent Screen)               | S34 |
| Figure S44: Raw GPC Data for Table S5 Entry 2   | S35 |
| Figure S45: Raw GPC Data for Table S5 Entry 3   | S35 |
| Figure S46: Raw GPC Data for Table S5 Entry 4   | S36 |
| Figure S47: Raw GPC Data for Table S5 Entry 5   | S36 |
| Figure S48: Raw GPC Data for Table S5 Entry 6   | S37 |
| Figure S49: Raw GPC Data for Table S5 Entry 7   | S37 |
| Figure S50: Raw GPC Data for Table S5 Entry 8   | S38 |
| Figure S51: Raw GPC Data for Table S5 Entry 9   | S38 |
| Figure S52: Raw GPC Data for Table S5 Entry 10  | S39 |
| Figure S53: Raw GPC Data for Table S6 Entry 1   | S39 |
| Figure S54: Raw GPC Data for Table S6 Entry 2   | S40 |
| Figure S55: Raw GPC Data for Table S6 Entry 3   | S40 |
| <b>7 References</b>   | S41 |

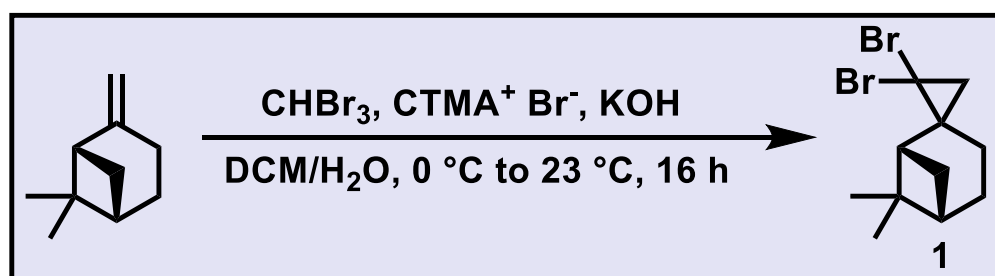
## 1 General Considerations

### 1.1 Materials and Methods

Unless otherwise noted, solvents were dried on an MBraun solvent purification system with 3Å molecular sieves and degassed with three freeze pump thaw cycles. All other reagents were obtained from commercial sources and used without further purification. Oxygen and water sensitive manipulations were performed in a nitrogen filled MBraun glovebox or using standard Schlenk techniques. All polymerizations were performed in a N<sub>2</sub> filled glovebox. <sup>1</sup>H and <sup>13</sup>C NMR data were collected on a Varian 600 MHz NMR, Varian 500 MHz NMR, or Varian 300 MHz NMR spectrometer. Chemical shifts (δ) are reported in ppm using the residual solvent as reference. Thermogravimetric analysis (TGA) was performed on a TA Instruments TGA Q500 and Dynamic Mechanical Analysis (DMA) data was collected on a TA Instruments DMA Q800 with a powder clamp. Gel Permeation Chromatography (GPC) data was collected on an Omnisec Resolve and Omisec Reveal System using triple detection with detectors in series: UV, light scattering, viscometer, and refractive index and three Viscotek styrene divinylbenzene copolymer columns (in series T3000, T4000, and T5000) at a flow rate of 1 mL/min and thermostatted to 30 °C using either tetrahydrofuran (THF) or chloroform (CHCl<sub>3</sub>) as the eluent. Molecular weight and dispersity data were determined using triple detection. Wide angle X-ray scattering (WAXS) of powder samples was performed on a Malvern Panalytical Empyrian X-ray diffractometer with a Cu anode and k(α) wavelength of 1.5406 Å.

## 2 Monomer Synthesis

### 2.1 Synthesis of **1**<sup>1,2</sup>

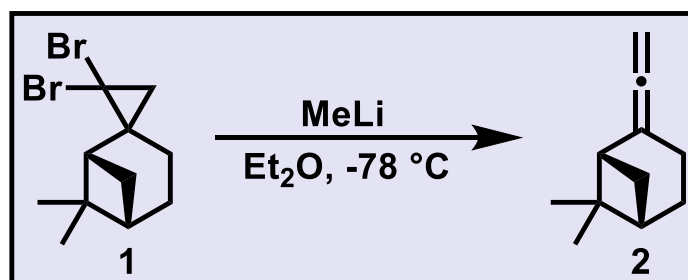


**Scheme S1:** Synthesis of **1**

A 500 mL round bottom flask was charged with a Teflon stir bar, (1S)-(-)-β-pinene (8.71 g, 63.86 mmol), dichloromethane (DCM, 100 mL), bromoform (CHBr<sub>3</sub>, 12.27 mL, 127.72 mmol), and cetyltrimethylammonium bromide (CTMA<sup>+</sup> Br<sup>-</sup>, 465.5 mg, 1.28 mmol). The mixture was cooled to 0 °C, and KOH (50% w/w in water) was added dropwise (21.5 g, 383.16 mmol). The resulting mixture was left to stir for 16 h while warming to room temperature. The reaction mixture was then neutralized with 2 M HCl and diluted with water (75 mL). The organic phase was separated, and the aqueous phase was extracted with DCM (2 x 50 mL). The combined organic layers were washed with brine (2 x 100 mL), dried over sodium sulfate, and filtered. The solvent was removed under vacuum,

after which the crude product was dissolved in hexanes and filtered through a plug of silica gel. Subsequent solvent removal under vacuum afforded **1** as a colorless oil (18.35 g, 93% yield). **<sup>1</sup>H NMR (300 MHz, CDCl<sub>3</sub>):** δ 2.51-2.36 (1H, m), 2.26 (1H, dt, J = 10 Hz, J = 6 Hz), 2.00-1.86 (4H, m), 1.58-1.48 (3H, m), 1.43-1.31 (1H, m), 1.24 (3H, s), 0.91 (3H, s). **<sup>13</sup>C NMR (75 MHz, CDCl<sub>3</sub>):** δ 50.13, 40.24, 40.08, 39.72, 26.88, 24.41, 26.06, 23.82, 21.78. Spectral data are shown in Figures S15 and S16.

## 2.2 Synthesis of **2**

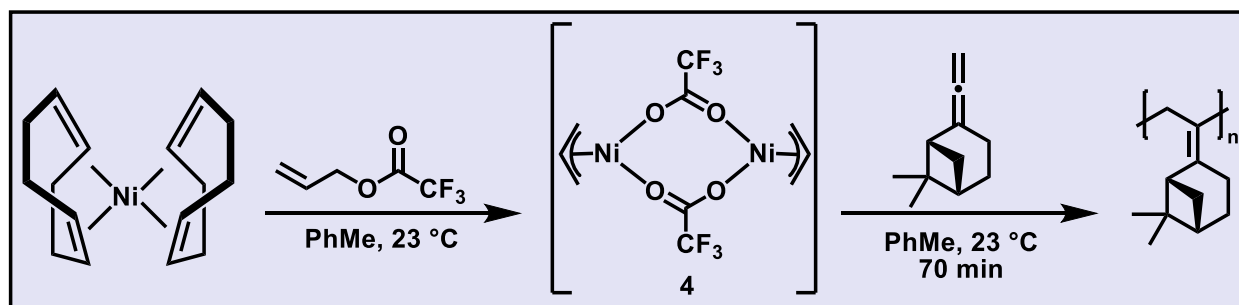


**Scheme S2:** Synthesis of **2**

A 100 mL flame dried Schlenk flask was charged with a Teflon stir bar, **1** (6.16 g, 20.00 mmol), and diethyl ether (Et<sub>2</sub>O, 40 mL) before cooling the solution to -78 °C (10 min isotherm). Methyllithium (1.6 M in Et<sub>2</sub>O, 14.40 mL, 23.04 mmol) was then added dropwise, and the reaction was stirred at -78 °C for 45 min. The reaction mixture was then warmed to 0 °C and quenched with water (15 mL). The mixture was then warmed to room temperature and further diluted with water (10 mL). The organic phase was separated, and the aqueous layer was extracted with Et<sub>2</sub>O (3 x 15 mL). The combined organic layers were washed with brine (2 x 20 mL), dried over sodium sulfate, filtered, and concentrated under vacuum. Vacuum distillation at 65 °C afforded **2** as a colorless oil (2.51 g, 84.7% yield). Spectral data were consistent with literature reports.<sup>1,2</sup> **2** was further characterized by <sup>13</sup>C, <sup>1</sup>H-<sup>1</sup>H COSY, and <sup>1</sup>H-<sup>13</sup>C HSQC NMR spectroscopy (see section 3.1.1 for additional details). Spectral data are shown in Figures S17 – S20.

## 3 Polymerization Studies and Material Characterization

### 3.1 General Procedure for the Vinyl-Addition Polymerization of **2** Using **4**



**Scheme S3:** Generation of **4** *in situ* and Synthesis of **3**

In an N<sub>2</sub> filled glovebox, bis(1,5-cyclooctadiene)nickel(0) (10 mg, 0.036 mmol) was dissolved in toluene (1.38 mL). To this solution was added allyltrifluoroacetate (4.7  $\mu$ L, 0.036 mmol), which generated **4** *in situ*. This freshly prepared stock solution of **4** ([Ni] = 0.026 M) was subsequently used in polymerization studies. An aliquot of the catalyst stock solution was added to a solution of **2** in toluene (0.25 M). The amount of catalyst solution added was dictated by the desired [2]<sub>0</sub>:[Ni]<sub>0</sub> ratios (Table S1). Polymerizations were conducted at 23 °C for 70 min unless otherwise noted in Table 1. Polymerizations were quenched by precipitation into methanol. The precipitated solids were filtered and then dried under vacuum. GPC data for the isolated polymers are reported in Figure S1. <sup>1</sup>H and <sup>13</sup>C NMR spectra for the precipitated material were collected in CDCl<sub>3</sub> (Figures S21 and S22).

**Table S1:** Selected Molecular Weight Data for **3**.

| Entry | [2] <sub>0</sub> :[Ni] <sub>0</sub> | <i>M<sub>n</sub></i> (Da) <sup>(a)</sup> | Target <i>M<sub>n</sub></i> <sup>(b)</sup> | $\bar{D}$ <sup>(c)</sup> |
|-------|-------------------------------------|--|--|--------------------------|
| 1     | 34:1                                | 7,504                                    | 5,040                                      | 1.37                     |
| 2     | 86:1                                | 18,920                                   | 12,750                                     | 1.19                     |
| 3     | 169:1                               | 26,420                                   | 25,050                                     | 1.13                     |
| 4     | 337:1                               | 52,030                                   | 49,960                                     | 1.23                     |
| 5     | 503:1                               | 66,270                                   | 74,570                                     | 1.23                     |
| 6     | 688:1                               | 99,580                                   | 102,000                                    | 1.31                     |

(a) Determined by GPC. (b) Calculated using [2]<sub>0</sub>:[Ni]<sub>0</sub> X 148.25 (rounded values shown). (c) Calculated using *M<sub>w</sub>*/*M<sub>n</sub>*.

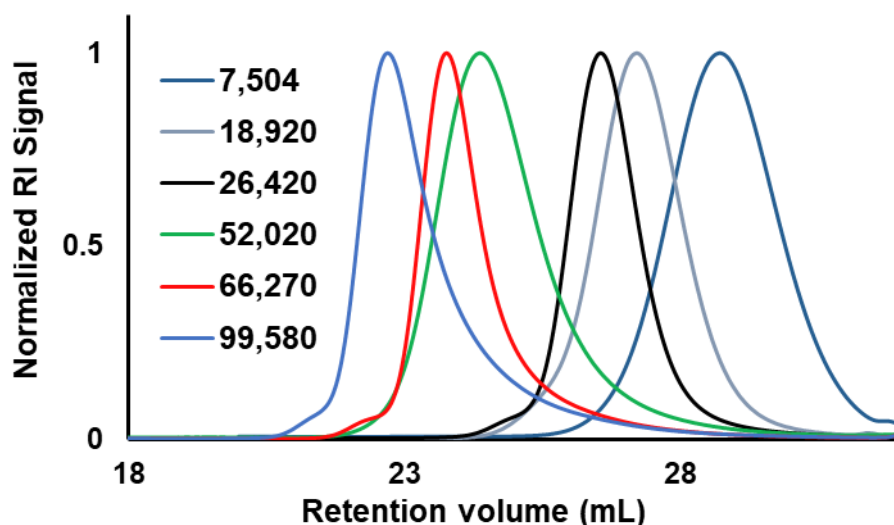


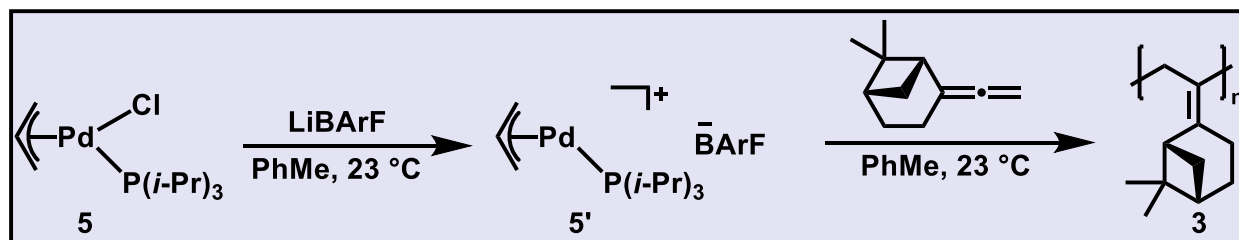
**Figure S1:** Selected GPC Data for **3**.

### 3.1.1 Confirmation of Fused-Ring Structure of **3**

The HSQC spectrum of **2** (Figure S19) shows the  $^1\text{H}$  resonances at  $\delta = 2.57$  and  $2.21$  (each of which integrates to 1H) correlate to the same  $^{13}\text{C}$  resonance at  $\delta = 19.60$ ; therefore, these protons represent a methylene set. The  $^1\text{H}$  resonances at  $\delta = 2.34$  and  $1.51$  (each of which integrates to 1H) correlate to the same  $^{13}\text{C}$  resonance at  $\delta = 26.14$ ; therefore, these protons represent another methylene set. Finally, the  $^1\text{H}$  resonances at  $\delta = 1.89$  and  $1.82$  (each of which integrates to 1H) correlate to the same  $^{13}\text{C}$  resonance at  $\delta = 23.67$ ; therefore, these protons represent another methylene set. The  $^1\text{H}$  resonances at  $\delta = 2.47$  and  $1.92$  each integrate to 1H and correlate to separate  $^{13}\text{C}$  resonances ( $\delta = 47.73$  and  $40.31$ , respectively); thus, these correspond to two methines. The COSY spectrum of **2** (Figure S20) shows a correlation between the methylene set at  $\delta = 2.57$  and  $2.21$  with the vinylic protons of the allene unit which can therefore be assigned as the methylene vicinal to the allene. The two methine protons were found to have correlations with the remaining two methylene sets, making the determination of the bridging methylene difficult. As such, the HSQC spectrum of **2** was found to be more diagnostic.

Due to significant broadening and overlap in the  $^1\text{H}$  and  $^{13}\text{C}$  NMR spectra of **3** ( $M_n = 79,910$  Da), COSY correlations were not as informative (Figure S23). However, the HSQC spectrum of **3** (Figure S24) clearly shows the retention of two methine protons (correlating to  $^{13}\text{C}$  resonances at  $\delta = 46.39$  and  $40.73$ , respectively); these correlations and chemical shifts are not consistent with the presence of an endocyclic olefin. Three methylene sets are also observed in the HSQC spectrum of **3**.

### 3.2 Procedure for the Vinyl-Addition Polymerization of **2** Using **5**



**Scheme S4:** Vinyl-Addition Polymerization of **2** Using **5**

In an  $\text{N}_2$  filled glovebox,  $(\eta^3\text{-allyl})\text{Pd}(i\text{-Pr}_3\text{P})\text{Cl}$  (**5**; 0.8 mg, 0.0022 mmol) and LiBARf (1.5 mg, 0.0022 mmol) were taken up in toluene (0.2 mL) and allowed to stir for 15 min to generate **5'** *in situ* ( $[\text{Pd}] = 0.011$  M). The solution of **5'** was then added to a solution of **2** (66 mg, 0.443 mmol). The reaction was allowed to stir at  $23^\circ\text{C}$  for 70 min, at which time the solution was added to methanol to precipitate any polymeric material. GPC data for the isolated polymer is reported in Figure S2.  $^1\text{H}$  NMR spectroscopic data for the precipitated material (collected in  $\text{CDCl}_3$ ; Figure S25) was consistent with that observed for the material prepared using **4**.

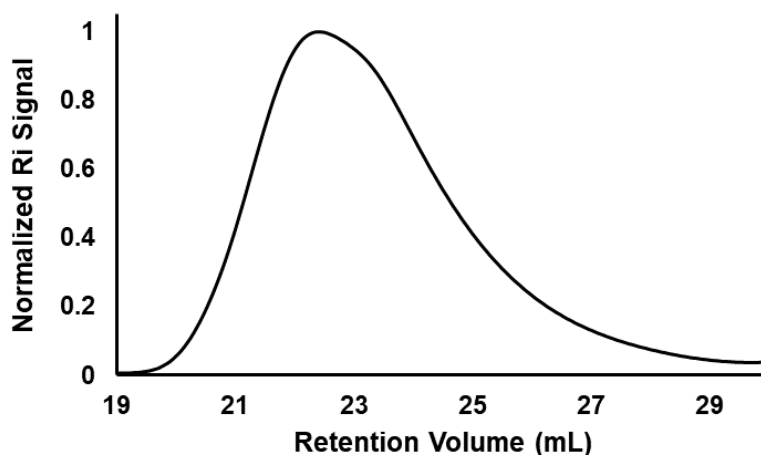
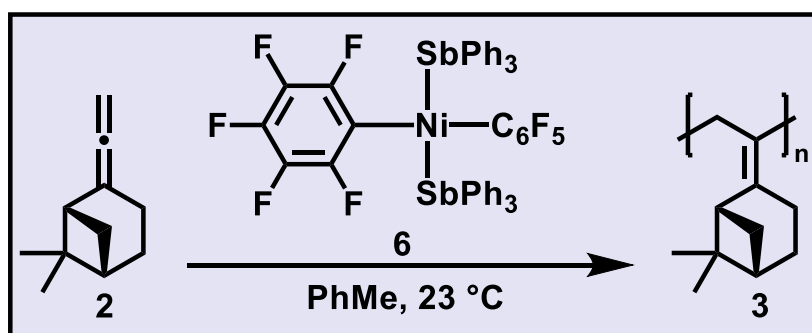


**Figure S2:** GPC Data for the Vinyl-Addition Polymerization of **2** Using **5'**

### 3.3 Procedure for the Vinyl-Addition Polymerization of **2** Using **6**



**Scheme S5:** Vinyl-Addition Polymerization of **2** Using **6**

In an N<sub>2</sub> filled glovebox, *trans*-[Ni(C<sub>6</sub>F<sub>5</sub>)<sub>2</sub>(SbPh<sub>3</sub>)<sub>2</sub>] (2.6 mg, 0.0024 mmol) was taken up in toluene (0.2 mL). The solution of **6** ([Ni] = 0.012 M) was then added to a solution of **2** (73 mg, 0.489 mmol). The reaction was allowed to stir at 23 °C for 70 minutes, at which point polymer product was recovered by precipitation in methanol. GPC data for the isolated polymer is reported in Figure S3. <sup>1</sup>H NMR spectroscopic data for the precipitated material (collected in CDCl<sub>3</sub>; Figure S26) was consistent with that observed for the material prepared using **4**.

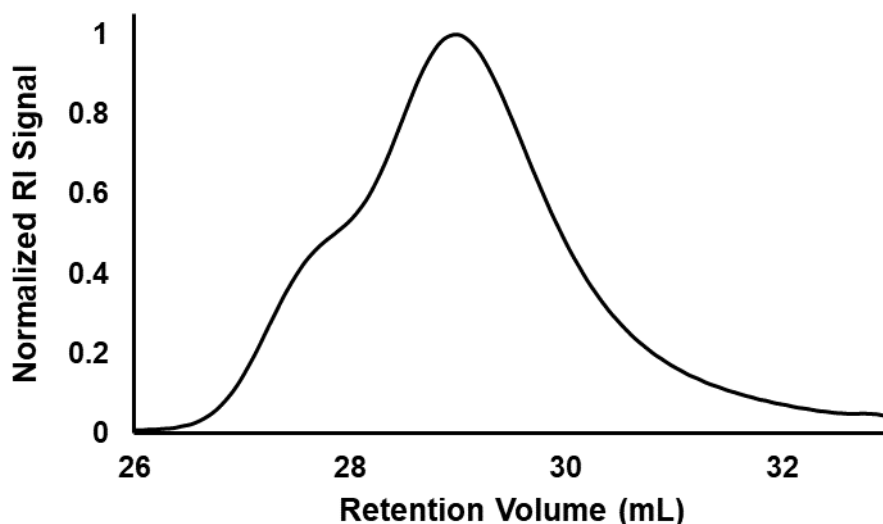


**Figure S3:** GPC Data for the Vinyl-Addition Polymerization of **2** Using **6**

### 3.4 Initiator Screen for Other Polymerizations of **2**

Polymerization of **2** was also attempted under uncontrolled radical (section 3.4.1), controlled radical (section 3.4.2), anionic (section 3.4.3), and cationic conditions (sections 3.4.4 and 3.4.5). All reactions were performed outside of the glovebox using standard Schlenk techniques.

#### 3.4.1 General Procedure for the Uncontrolled Radical Polymerization of **2**

A flame dried, septum capped 2-dram vial was charged with a Teflon stir bar, **2** (100 mg 0.675 mmol), THF (2.0 mL), and AIBN (0.17 mg, 0.001 mmol). The resulting solution was subjected to three freeze-pump-thaw cycles and allowed to warm to room temperature under an atmosphere of N<sub>2</sub>. Polymerizations were attempted under a variety of temperatures and times (Table S2); however, no polymeric product was recovered upon addition of the reaction mixtures to methanol.

#### 3.4.2 General Procedure for the Controlled Radical Polymerization of **2**

A flame dried, septum capped 2-dram vial was charged with a Teflon stir bar wrapped in copper wire, **2** (100 mg, 0.675 mmol), DMSO (2.0 mL), ethyl  $\alpha$ -bromoisobutyrate (0.20 mg, 0.001 mmol), and PMDETA (50  $\mu$ L, 7.19 mmol). The resulting solution was subjected to three freeze-pump-thaw cycles and allowed to warm to room temperature under an atmosphere of N<sub>2</sub>. Polymerizations were attempted under a variety of temperatures and times (Table S2); however, no polymeric product was recovered upon addition of the reaction mixtures to methanol.

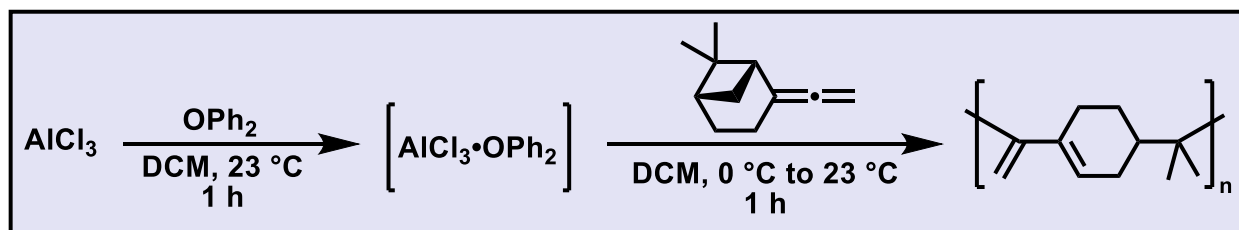
### 3.4.3 General Procedure for the Anionic Polymerization of **2**

A flame dried 10 mL Schlenk flask was charged with a Teflon stir bar, **2** (150 mg, 1.01 mmol), and Et<sub>2</sub>O (4 mL). The solution was cooled to 0 °C, and an alkyl lithium solution in Et<sub>2</sub>O (0.0075 mmol lithiate; Table S2) was added. The reaction was then allowed to stir under an atmosphere on N<sub>2</sub> for 1 h. Polymerizations were attempted with a variety of alkyl lithiates under various temperatures (Table S2); however, no polymeric product was recovered upon addition of the reaction mixtures to methanol.

### 3.4.4 General Procedure for the Cationic Polymerization of **2**

A flame dried, septum capped 2-dram vial was charged with a Teflon stir bar, **2** (150 mg, 1.01 mmol), and solvent (4 mL; see Table S2). In a separate flame dried, septum capped 2-dram vial, a 0.15 M stock solution of cationic initiator was prepared (Table S2). The solution of **2** was cooled to 0 °C, and the initiator solution was added via syringe. Reactions were carried out under an atmosphere of N<sub>2</sub> while warming from 0 → 23 °C over the course of 1 h. Polymeric product was recovered from methanol precipitation only in the case of polymerizations mediated by AlCl<sub>3</sub>•OPh<sub>2</sub> (Table S2, entry 12; see section 3.4.5 for additional details).

### 3.4.5 Cationic Ring-Opening Polymerization of **2** with AlCl<sub>3</sub>•OPh<sub>2</sub>



**Scheme S6:** Cationic Ring-Opening Polymerization of **2** with AlCl<sub>3</sub>•OPh<sub>2</sub>

The cationic ring-opening polymerization of **2** was performed according to a modification of the procedure developed by Kostjuk.<sup>3</sup> A flame dried, septum capped 2-dram vial was charged with a Teflon stir bar and AlCl<sub>3</sub> (74 mg, 0.55 mmol). The AlCl<sub>3</sub> was suspended in DCM (3.7 mL), and diphenyl ether (87.5 μL, 0.55 mmol) was added dropwise. The mixture was stirred for 1 h to generate a 0.15 M solution of the AlCl<sub>3</sub>•OPh<sub>2</sub> complex. In a separate vial, **2** (140 mg, 0.94 mmol) was taken up in DCM (0.25 M) and cooled to 0 °C. The AlCl<sub>3</sub>•OPh<sub>2</sub> solution (50 μL, 0.075 mmol) was then added via syringe to the solution of **2**, and the mixture was allowed to stir from 0 °C → 23 °C over a period of 1 h. The polymer product was recovered by precipitation in methanol (26.3 mg, 18.8% yield). GPC data for the isolated polymer is reported in Figure S4. <sup>1</sup>H NMR spectroscopic analysis of the precipitated material (collected in CDCl<sub>3</sub>; Figure S27) revealed two sets of vinyl signals (δ = 5.61 and δ = 6.56), which was interpreted as evidence of ring-opening during the polymerization.

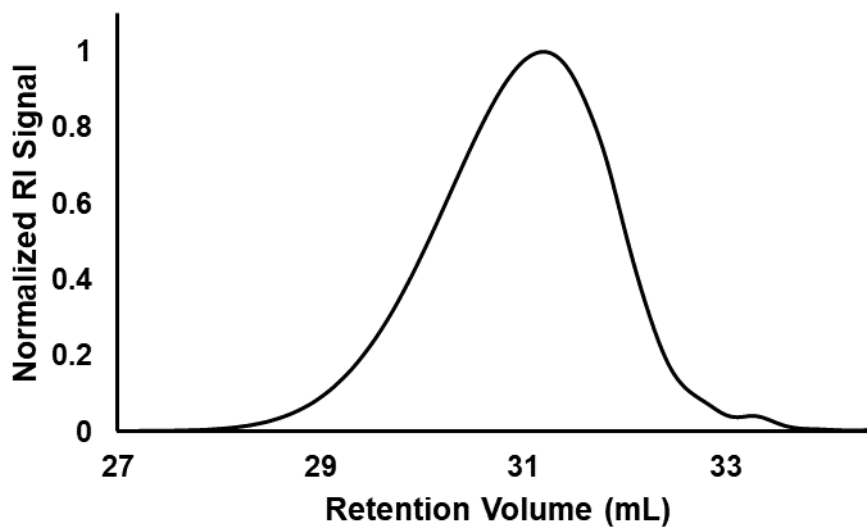
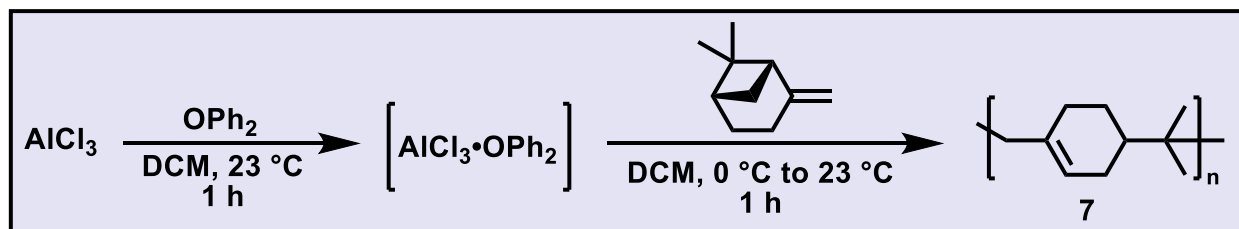


**Figure S4:** GPC Data for the Cationic Ring-Opening Polymerization of **2**

**Table S2:** Initiator Screen for the Ring-opening Polymerization of **2**

| Entry | Initiator                           | Solvent           | [2] <sub>0</sub> : [Initiator] <sub>0</sub> | Time (h) | Temperature (°C) | Yield (%) |
|-------|-------------------------------------|-------------------|---|----------|------------------|-----------|
| 1     | AIBN                                | THF               | 650:1                                       | 16       | 80               | 0         |
| 2     | AIBN                                | THF               | 650:1                                       | 24       | 80               | 0         |
| 3     | AIBN                                | THF               | 650:1                                       | 16       | 90               | 0         |
| 4     | Bromoisobutyrate (Cu/PMDETA)        | DMSO              | 650:1                                       | 16       | 23               | 0         |
| 5     | Bromoisobutyrate (Cu/PMDETA)        | DMSO              | 650:1                                       | 16       | 50               | 0         |
| 6     | MeLi                                | Et <sub>2</sub> O | 130:1                                       | 1        | 0                | 0         |
| 7     | MeLi                                | Et <sub>2</sub> O | 130:1                                       | 1        | 23               | 0         |
| 8     | n-BuLi                              | Et <sub>2</sub> O | 130:1                                       | 1        | 0                | 0         |
| 9     | n-BuLi                              | Et <sub>2</sub> O | 130:1                                       | 1        | 23               | 0         |
| 10    | BF <sub>3</sub> OMe <sub>2</sub>    | Et <sub>2</sub> O | 140:1                                       | 1        | 0 – 23           | 0         |
| 11    | AlCl <sub>3</sub>                   | DCM               | 12.5:1                                      | 1        | 0 – 23           | 0         |
| 12    | AlCl <sub>3</sub> •OPh <sub>2</sub> | DCM               | 12.5:1                                      | 1        | 0 – 23           | 18.8      |

### 3.5 Procedure for the Preparation of **7**



**Scheme S7:** Preparation of **7**

**7** was prepared according to a modification of the procedure developed by Kostjuk.<sup>3</sup>  $\text{AlCl}_3\bullet\text{OPh}_2$  was prepared according to the procedure described in section 3.4.5. In a separate flame dried Schlenk flask, (1S)-(-)- $\beta$ -pinene (6.54 g, 36.7 mmol) was taken up in DCM/hexanes (21 mL:14 mL) and cooled to 0 °C. The  $\text{AlCl}_3\bullet\text{OPh}_2$  solution (0.75 mL, 0.11 mmol) was then added to via syringe, and the resulting mixture was allowed to stir at 0 °C for 2 min. After warming to room temperature, the solution was added to methanol to precipitate any polymeric material. Filtration of these solids afforded **7** as a white powder (1.08 g, 21.6% yield). GPC data for the isolated polymer is reported in Figure S5.  $^1\text{H}$  and  $^{13}\text{C}$  NMR spectra of the precipitated material was consistent with literature values<sup>3–5</sup> (Figures S28 and S29).

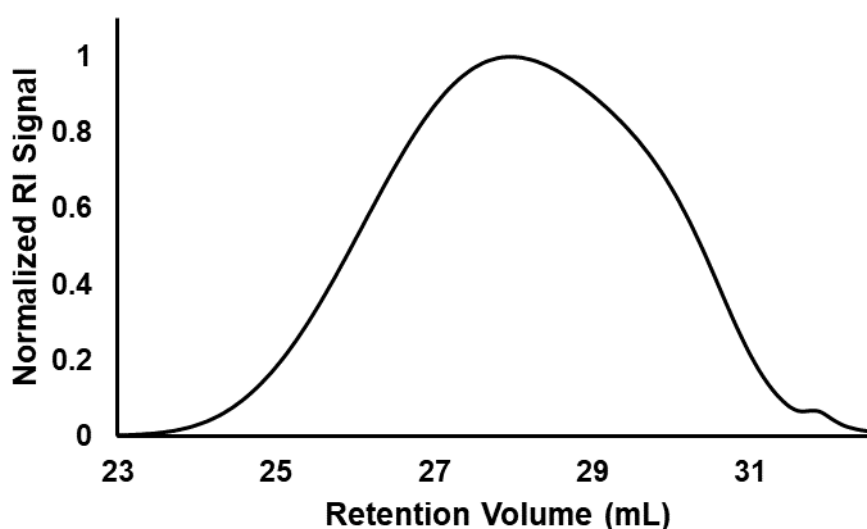


**Figure S5:** GPC Data for **7**

### 3.6 Thermomechanical Data

TGA thermograms were collected using powder samples of **3** and **7** (10 °C/min heating rate). Powder samples of **3** and **7** were analyzed by DMA using a powder clamp attachment. Samples were heated at a rate of 2 °C/min at 1.00 Hz.

#### 3.6.1 TGA and DMA Data for **3**

Representative thermomechanical data for **3** ( $M_n = 7,504$  Da) are shown in Figures S6 and S7. The TGA thermogram of a powdered sample revealed an initial decomposition onset temperature of 294 °C (Figure S6). Negligible mass loss was observed below this temperature. A powder sample of the same polymer exhibited a peak in  $\text{Tan}\delta$  at 160 °C (Figure S7) when analyzed by DMA.

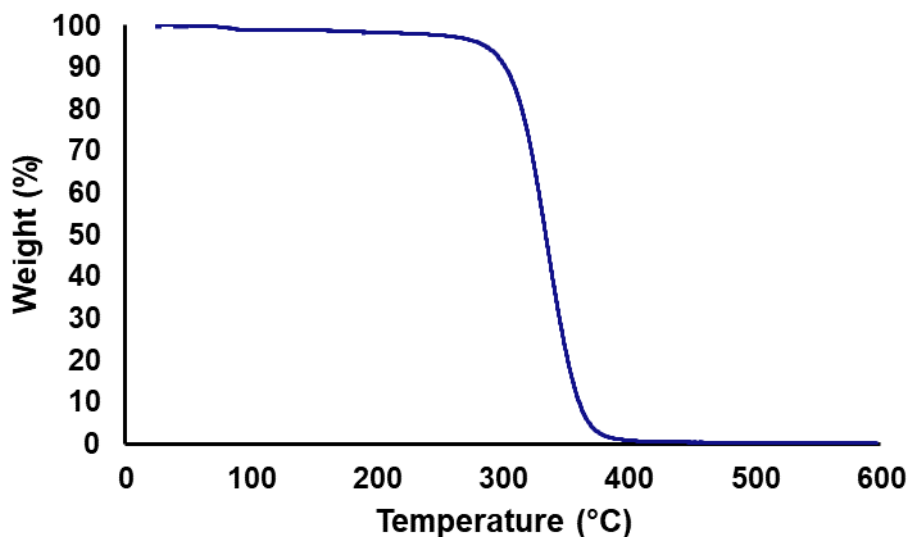


**Figure S6:** Representative TGA Thermogram of **3** (10 °C/min heating rate)

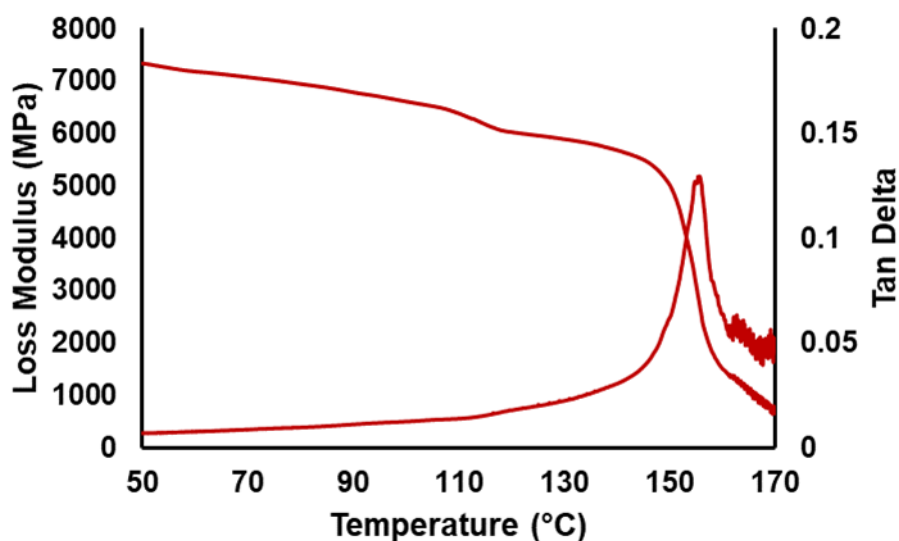


**Figure S7:** Representative Powder DMA of **3** (2 °C/min; 1.00 Hz)

### 3.6.2 TGA and DMA Data for **7**

Representative thermomechanical data for **7** ( $M_n = 5,812$  Da) are shown in Figures S8 and S9. The TGA thermogram of a powdered sample indicated an initial decomposition onset temperature of 303 °C (Figure S8). Negligible mass loss was observed below this temperature. A powder sample of the same polymer revealed a peak in  $\text{Tan}\delta$  at 82 °C when analyzed by DMA (Figure S9).

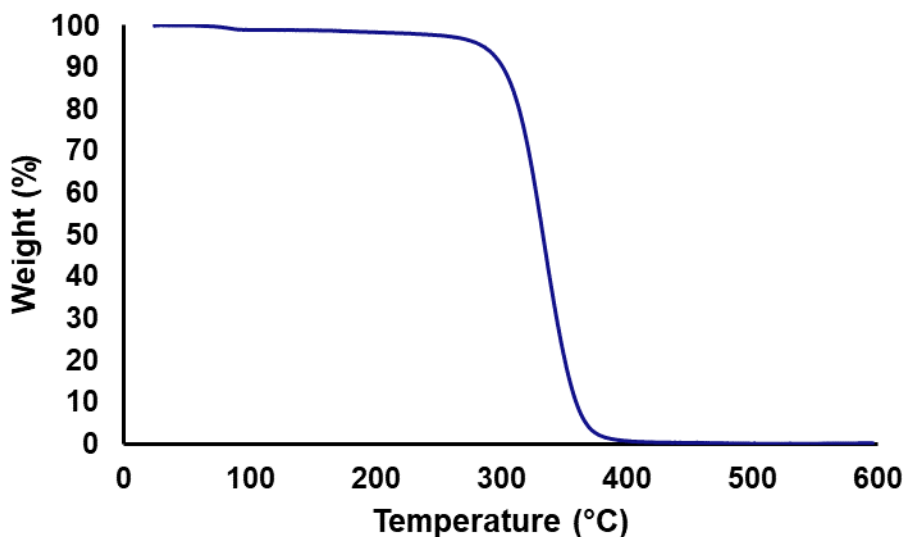


**Figure S8:** Representative TGA Thermogram of **7** (10 °C/min heating rate)

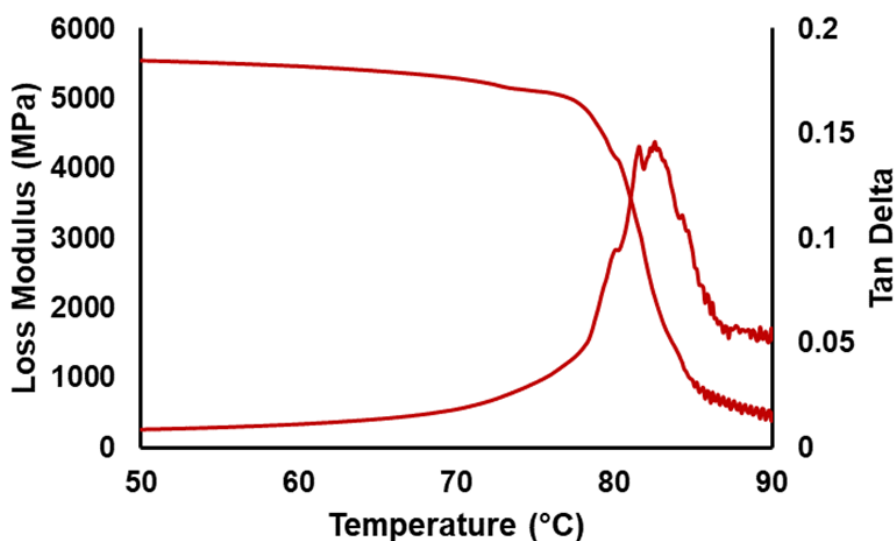


**Figure S9:** Representative Powder DMA of **7** (2 °C/min; 1.00 Hz)

### 3.6.3 WAXS Measurements of **3**

WAXS was performed on low molecular weight ( $M_n = 7,504$  Da) and high molecular weight ( $M_n = 79,910$  Da) powder samples of **3**. WAXS was also performed on a powder sample of **7**, as well as annealed samples of **3** and **7**. WAXS measurements typically required 75 mg of polymer sample; comprehensive measurement parameters are given in Figures S10–12 and S13–14.

Freshly precipitated powder samples of **3** (both low and high molecular weight materials; Figures S10 and S11, respectively) displayed semi-crystalline peaks at  $2\theta = 7.45^\circ$  and  $15.52^\circ$  (averaged from low and high molecular weight materials). A sample of **3** ( $M_n =$

66,090 Da) was annealed for 1 h at 185 °C in a vacuum oven (Figure S12); WAXS analysis revealed similar semi-crystalline peaks at  $2\theta = 7.71^\circ$  and  $15.64^\circ$ . The d-spacing values for all materials were calculated using Bragg's law. Crystallite sizes were calculated using the Scherrer equation (shape factor value of 0.9 and instrumental line broadening of  $0.026^\circ$ ; results are summarized in Table S3). All calculations were performed following a baseline correction of the raw data file (second derivatives used as anchor points for baseline correction).

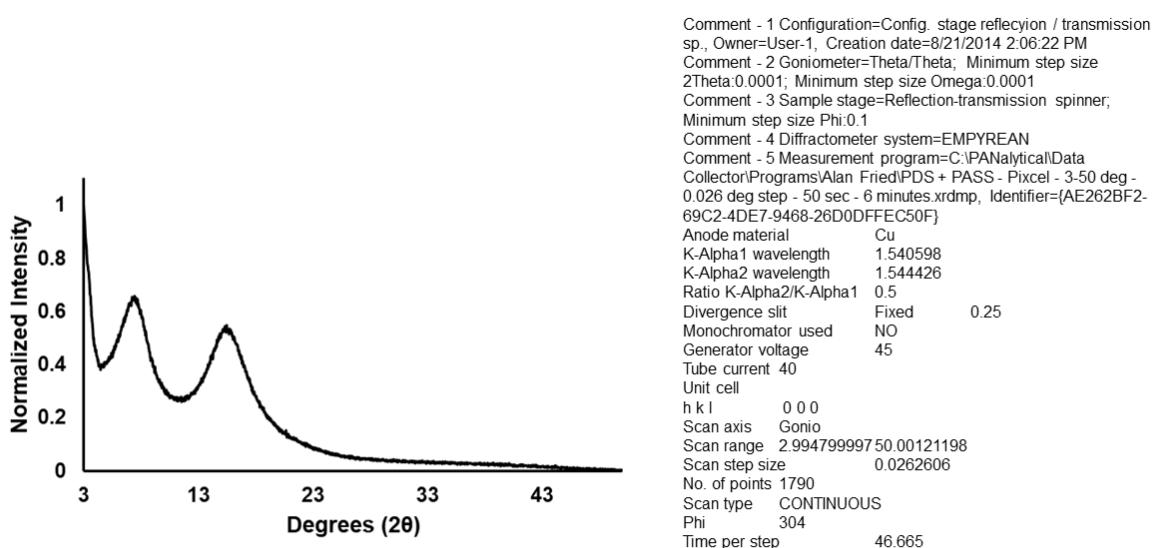


**Figure S10:** WAXS Spectrum of Low Molecular Weight ( $M_n = 7,504$  Da) 3

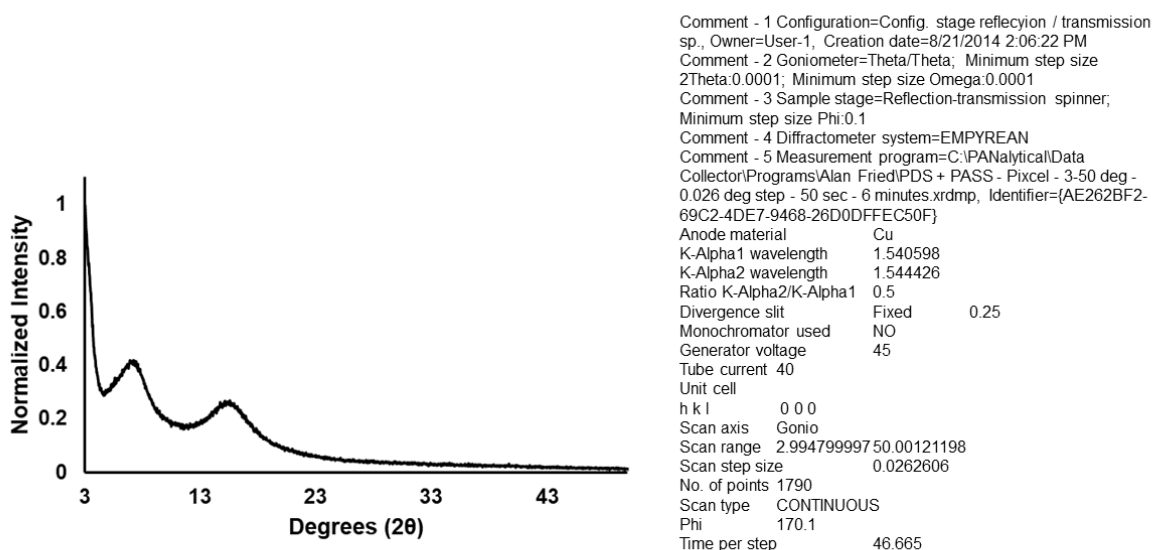


**Figure S11:** WAXS Spectrum of High Molecular Weight ( $M_n = 79,910$  Da) 3

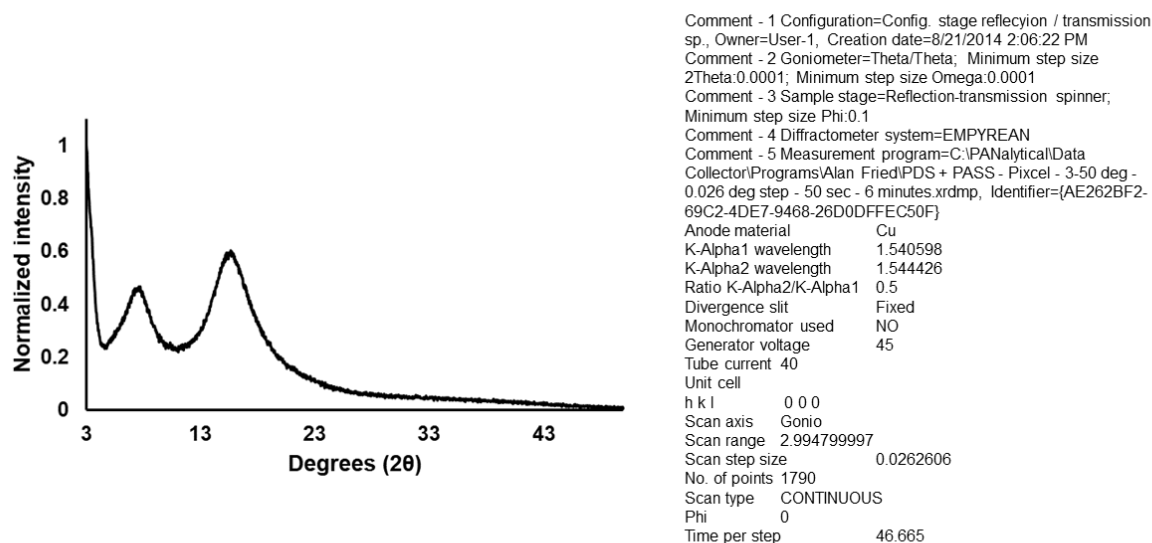


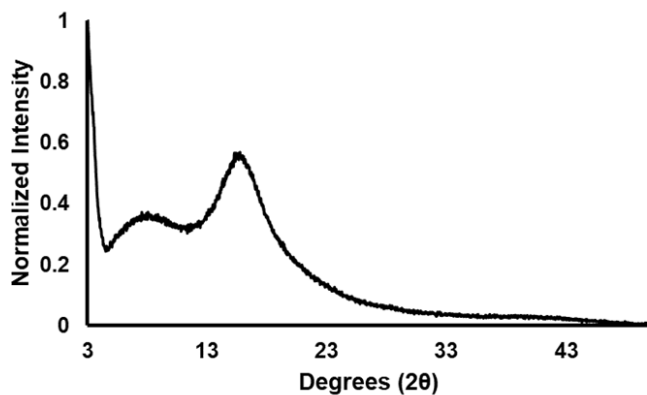
**Figure S12:** WAXS spectrum of Annealed **3** ( $M_n = 66,090$  Da)

**Table S3:** WAXS Data for **3**

|                     | Low angle peak |           |             | High angle peak |           |             |
|---------------------|----------------|-----------|-------------|-----------------|-----------|-------------|
|                     | Angle          | d-spacing | Crystallite | Angle           | d-spacing | Crystallite |
|                     | ( $2\theta$ )  | (nm)      | (Å)         | ( $2\theta$ )   | (nm)      | (Å)         |
| <b>3</b> (7.5 kDa)  | 7.45           | 11.86     | 32.4        | 15.48           | 5.72      | 22.6        |
| <b>3</b> (79.9 kDa) | 7.45           | 11.85     | 33.4        | 15.57           | 5.69      | 21.7        |
| <b>Annealed 3</b>   | 7.71           | 11.46     | 34.3        | 15.64           | 5.66      | 23.0        |

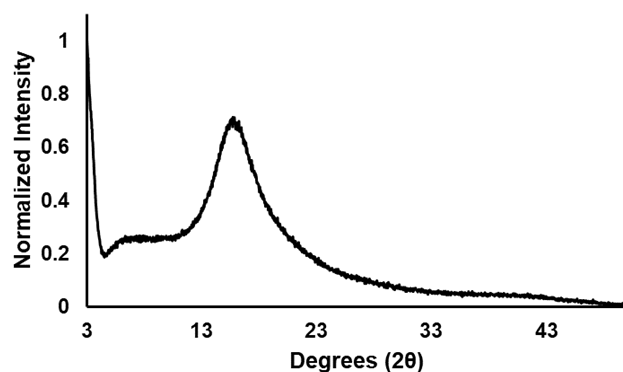
### 3.6.4 WAXS Measurements of **7**

WAXS analysis of a powder sample of **7** ( $M_n = 5,812$  Da; Figure S13) displayed an amorphous peak at  $2\theta = 7.52^\circ$  and a semi-crystalline peak at  $15.74^\circ$ . A separate sample of **7** ( $M_n = 6,151$  Da) was annealed for 1 h at  $105^\circ\text{C}$  in a vacuum oven (Figure S14); WAXS analysis revealed an amorphous peak at  $2\theta = 6.34^\circ$  and a semi-crystalline peak at  $15.85^\circ$ . The d-spacing values for all materials were calculated using Bragg's law. Crystallite sizes were calculated using the Scherrer equation (shape factor value of 0.9 and instrumental line broadening of  $0.026^\circ$ ; results are summarized in Table S4). All calculations were performed following a baseline correction of the raw data file (second derivatives used as anchor points for baseline correction)



Comment - 1 Configuration=Config. stage reflection / transmission  
 sp., Owner=User-1, Creation date=8/21/2014 2:06:22 PM  
 Comment - 2 Goniometer=Theta/Theta; Minimum step size  
 2Theta:0.0001; Minimum step size Omega:0.0001  
 Comment - 3 Sample stage=Reflection-transmission spinner;  
 Minimum step size Phi:0.1  
 Comment - 4 Diffractometer system=EMPYREAN  
 Comment - 5 Measurement program=C:\PANalytical\Data  
 Collector\Programs\Alan Fried\PDS + PASS - Pixel - 3-50 deg -  
 0.026 deg step - 50 sec - 6 minutes.xrdmp, Identifier={AE262BF2-  
 69C2-4DE7-9468-26D0DFFEC50F}  
 Anode material Cu  
 K-Alpha1 wavelength 1.540598  
 K-Alpha2 wavelength 1.544426  
 Ratio K-Alpha2/K-Alpha1 0.5  
 Divergence slit Fixed 0.25  
 Monochromator used NO  
 Generator voltage 45  
 Tube current 40  
 Unit cell  
 h k l 0 0 0  
 Scan axis Gonio  
 Scan range 2.994799997 50.00121198  
 Scan step size 0.0262606  
 No. of points 1790  
 Scan type CONTINUOUS  
 Phi 21  
 Time per step 46.665

**Figure S13: WAXS Spectrum of 7 ( $M_n = 5,812$  Da)**



Comment - 1 Configuration=Config. stage reflection / transmission  
 sp., Owner=User-1, Creation date=8/21/2014 2:06:22 PM  
 Comment - 2 Goniometer=Theta/Theta; Minimum step size  
 2Theta:0.0001; Minimum step size Omega:0.0001  
 Comment - 3 Sample stage=Reflection-transmission spinner;  
 Minimum step size Phi:0.1  
 Comment - 4 Diffractometer system=EMPYREAN  
 Comment - 5 Measurement program=C:\PANalytical\Data  
 Collector\Programs\Alan Fried\PDS + PASS - Pixel - 3-50 deg -  
 0.026 deg step - 50 sec - 6 minutes.xrdmp, Identifier={AE262BF2-  
 69C2-4DE7-9468-26D0DFFEC50F}  
 Anode material Cu  
 K-Alpha1 wavelength 1.540598  
 K-Alpha2 wavelength 1.544426  
 Ratio K-Alpha2/K-Alpha1 0.5  
 Divergence slit Fixed 0.25  
 Monochromator used NO  
 Generator voltage 45  
 Tube current 40  
 Unit cell  
 h k l 0 0 0  
 Scan axis Gonio  
 Scan range 2.994799997 50.00121198  
 Scan step size 0.0262606  
 No. of points 1790  
 Scan type CONTINUOUS  
 Phi 221.4  
 Time per step 46.665

**Figure S14: WAXS Spectrum of Annealed 7 ( $M_n = 6,151$  Da)**

**Table S4:** WAXS Data for **7**

|                     | Low angle peak |              |             | High angle peak |             |             |
|---------------------|----------------|--------------|-------------|-----------------|-------------|-------------|
|                     | Angle          | d-spacing    | Crystallite | Angle           | d-spacing   | Crystallite |
|                     | (2 $\theta$ )  | (nm)         | (Å)         | (2 $\theta$ )   | (nm)        | (Å)         |
| <b>7 (5.81 kDa)</b> | <b>7.52</b>    | <b>11.74</b> | <b>21.4</b> | <b>15.74</b>    | <b>5.62</b> | <b>23.6</b> |
| <b>Annealed 7</b>   | <b>6.34</b>    | <b>13.92</b> | <b>n/a</b>  | <b>15.85</b>    | <b>5.59</b> | <b>20.5</b> |

#### 4 Determination of Living Character for the Polymerization of **2** Using **4**

##### 4.1 Molecular Weight as a Function of Monomer Conversion

In an N<sub>2</sub> filled glovebox, a stock solution of **4** was prepared according to the procedure outlined in section 3.1 ([Ni] = 0.026 M). In a separate vial, **2** (200 mg, 1.35 mmol) and mesitylene (as an internal standard; 188  $\mu$ L, 1.35 mmol) were taken up in toluene-d<sub>8</sub> (4.05 mL). A 0.26 mL (0.007 mmol in Ni) aliquot of the stock solution of **4** was added, and the reaction was allowed to stir at 23 °C. Aliquots (0.15 mL) of the reaction mixture were removed every 5 minutes, quenched by exposure to air, and analyzed using <sup>1</sup>H NMR spectroscopy. The aliquots were then concentrated to dryness and analyzed by GPC to determine the number average molecular weight ( $M_n$ ) of any polymeric species (Table S5). The calculated  $M_n$  data were plotted as a function of monomer conversion, which revealed a linear correlation (Figure 2A).

**Table S5:** Living Plot Molecular Weight and Conversion Data

| Entry     | Reaction Time<br>(min) | Conversion<br>(%) | $M_n$ (Da)    | $\bar{D}$   |
|-----------|------------------------|-------------------|---------------|-------------|
| <b>1</b>  | <b>0</b>               | <b>0</b>          | <b>-</b>      | <b>-</b>    |
| <b>2</b>  | <b>5</b>               | <b>36</b>         | <b>8,734</b>  | <b>1.27</b> |
| <b>3</b>  | <b>10</b>              | <b>42</b>         | <b>13,110</b> | <b>1.20</b> |
| <b>4</b>  | <b>15</b>              | <b>49</b>         | <b>15,150</b> | <b>1.20</b> |
| <b>5</b>  | <b>20</b>              | <b>58</b>         | <b>16,160</b> | <b>1.21</b> |
| <b>6</b>  | <b>25</b>              | <b>64</b>         | <b>17,260</b> | <b>1.23</b> |
| <b>7</b>  | <b>30</b>              | <b>72</b>         | <b>20,060</b> | <b>1.20</b> |
| <b>8</b>  | <b>35</b>              | <b>76</b>         | <b>20,690</b> | <b>1.20</b> |
| <b>9</b>  | <b>40</b>              | <b>80</b>         | <b>22,120</b> | <b>1.22</b> |
| <b>10</b> | <b>45</b>              | <b>86</b>         | <b>23,170</b> | <b>1.20</b> |

##### 4.2 Chain Extension Experiment

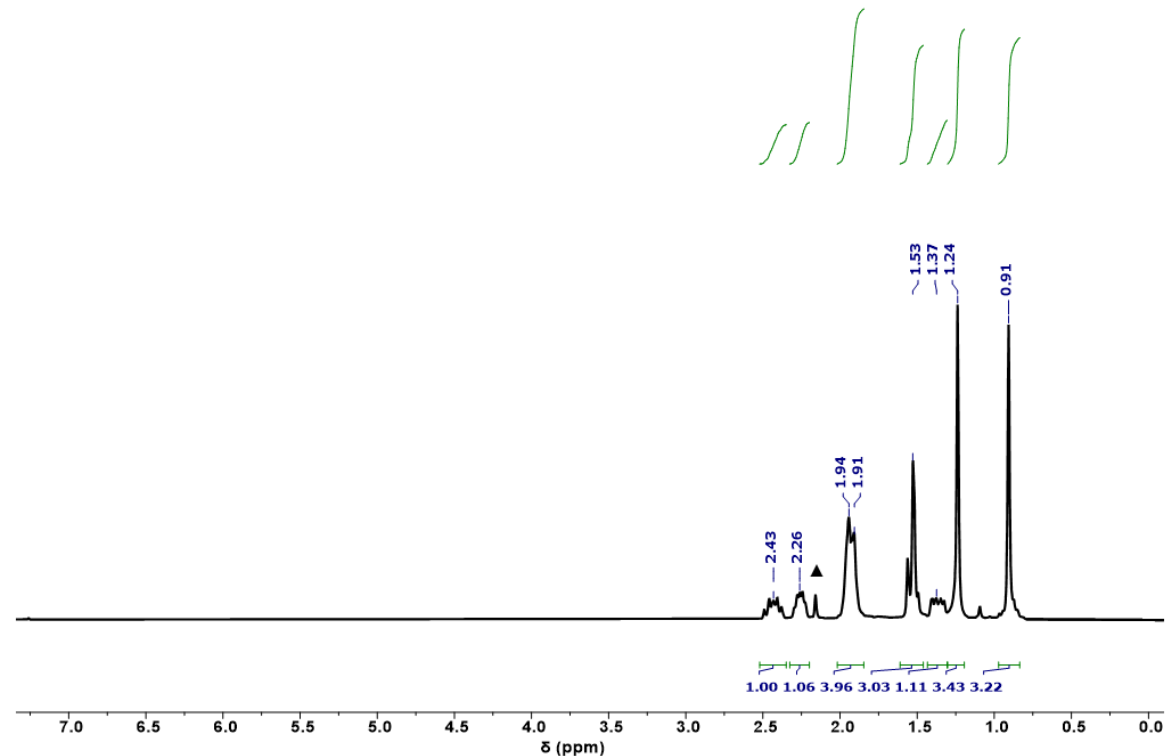
In an N<sub>2</sub> filled glovebox, a stock solution of **4** was prepared according to the procedure in section 3.1 ([Ni] = 0.026 M). In a separate vial, **2** (150 mg, 1.01 mmol) and mesitylene (as an internal standard; 140.5  $\mu$ L; 1.01 mmol) were taken up in toluene (7.0 mL). To the solution of **2**, a 0.385 mL aliquot of the stock solution of **4** was added (0.01 mmol Ni), and

the reaction was allowed to stir at 23 °C. After 70 min, a 0.2 mL aliquot of the reaction mixture was removed to confirm complete consumption of **2** by  $^1\text{H}$  NMR spectroscopy. At this point, a 150 mg (1.01 mmol) portion of **2** in 0.2 mL of toluene was added to the polymerization mixture and allowed to stir. Another 0.2 mL aliquot was taken after 70 min, and  $^1\text{H}$  NMR spectroscopic analysis revealed complete consumption of **2**. Finally, a second 150 mg (1.01 mmol) portion of **2** in 0.2 mL of toluene was added to the polymerization mixture and allowed to stir. Another 0.2 mL aliquot was taken after 70 min, and  $^1\text{H}$  NMR spectroscopic analysis revealed complete consumption of **2**. All NMR aliquots were concentrated under vacuum and analyzed by GPC to determine the number average molecular weight ( $M_n$ ) of any polymeric species (Table S6). Note: we calculated mmol Ni removed in each aliquot and iteratively subtracted this from the original total (0.01 mmol Ni). For each extension, we used this calculated mmol Ni, the measured  $M_n$  from the previous extension, and the amount of added monomer to determine target  $M_n$ . The observed data were consistent with successful chain extension (Figure 2B).

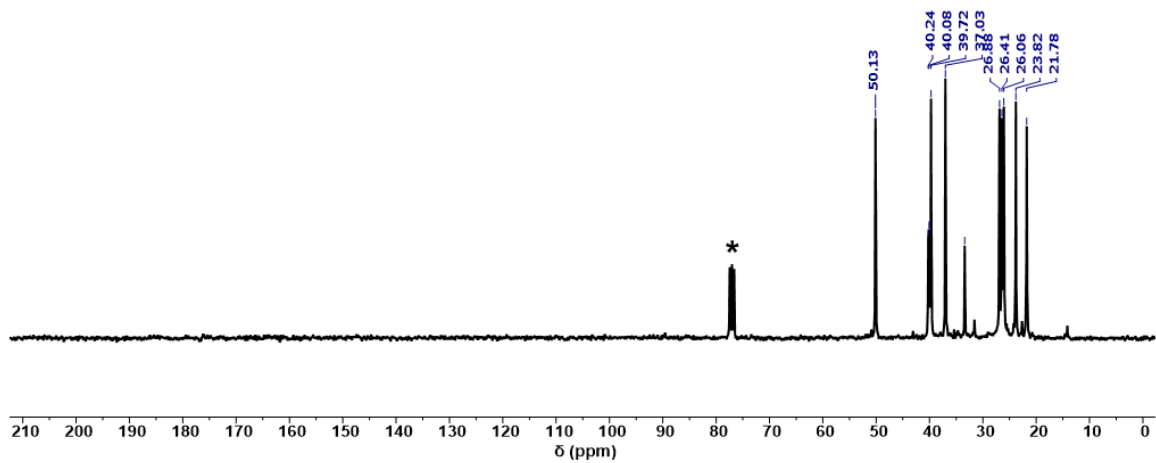
**Table S6:** Molecular Weight Data for Chain Extension of **3**

| Entry | Extensions | $M_n$ (Da) | Target $M_n$ (Da) | $\bar{D}$ |
|-------|------------|------------|-------------------|-----------|
| 1     | 0          | 28,530     | 14,973            | 1.30      |
| 2     | 1          | 45,420     | 43,920            | 1.30      |
| 3     | 2          | 59,590     | 61,238            | 1.36      |

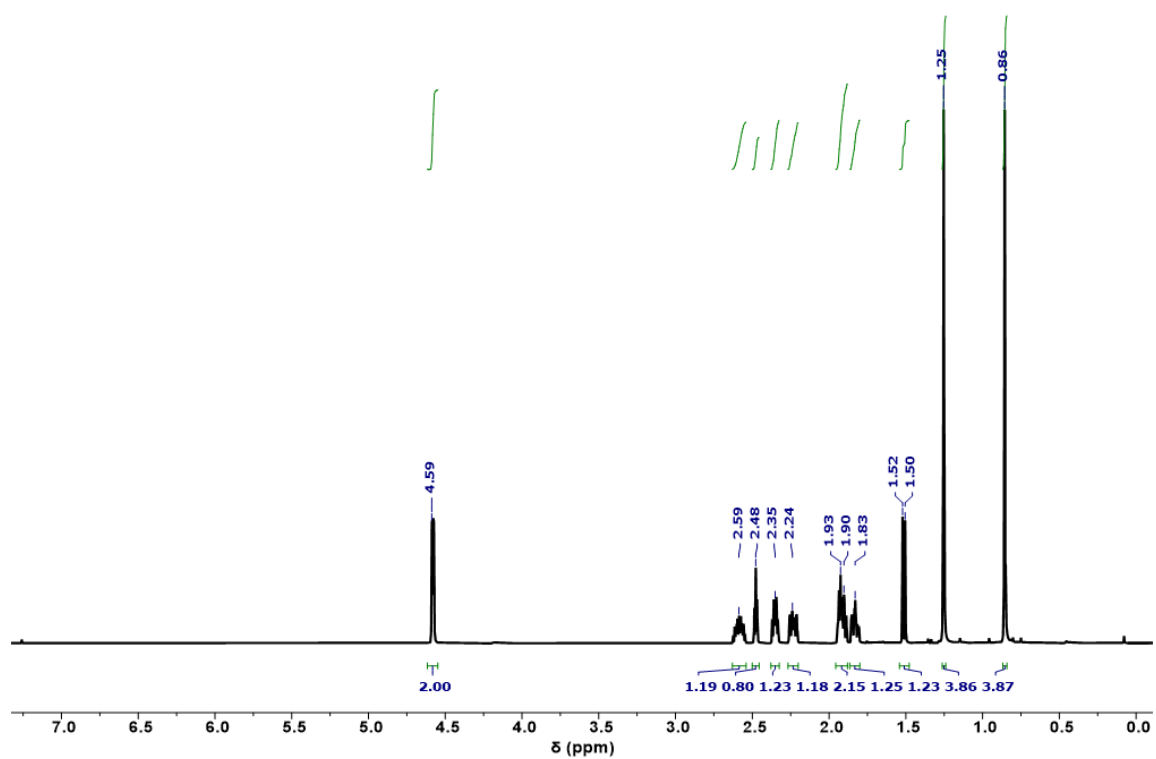
## 5 NMR Spectroscopic Data



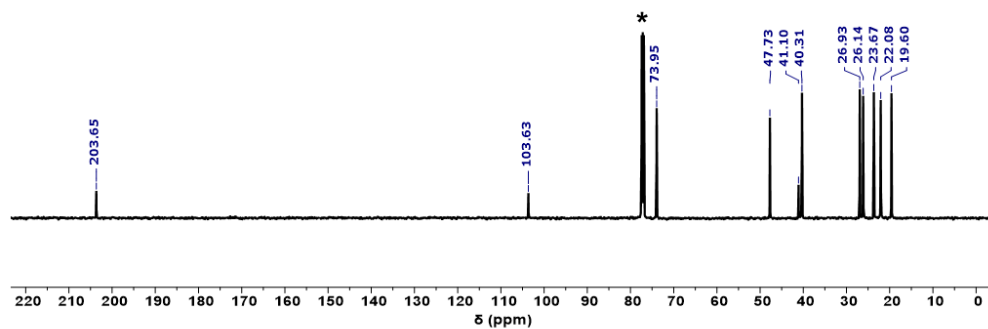
**Figure S15:**  $^1\text{H}$  NMR Spectrum of **1**. Residual Acetone Represented by ▲.



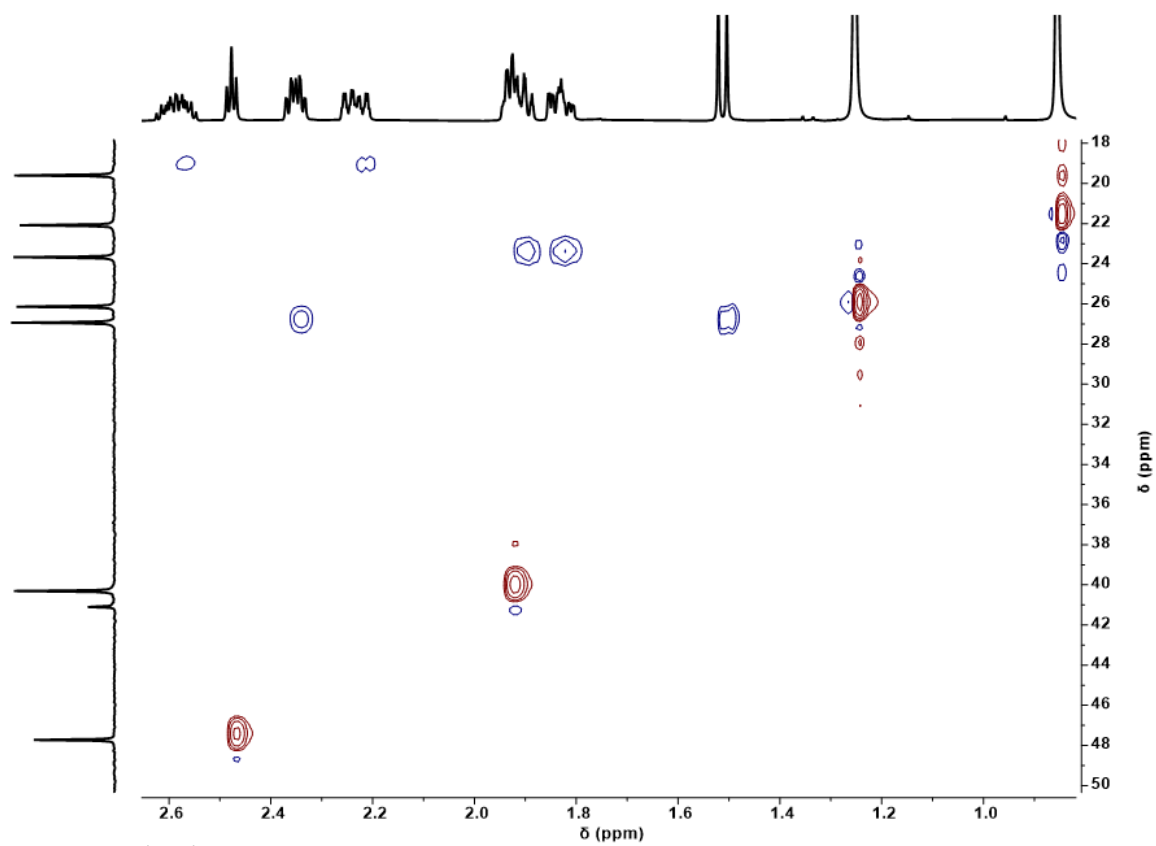
**Figure S16:**  $^1\text{H}$  NMR Spectrum of **1**.  $\text{CDCl}_3$  Resonance Represented by \*



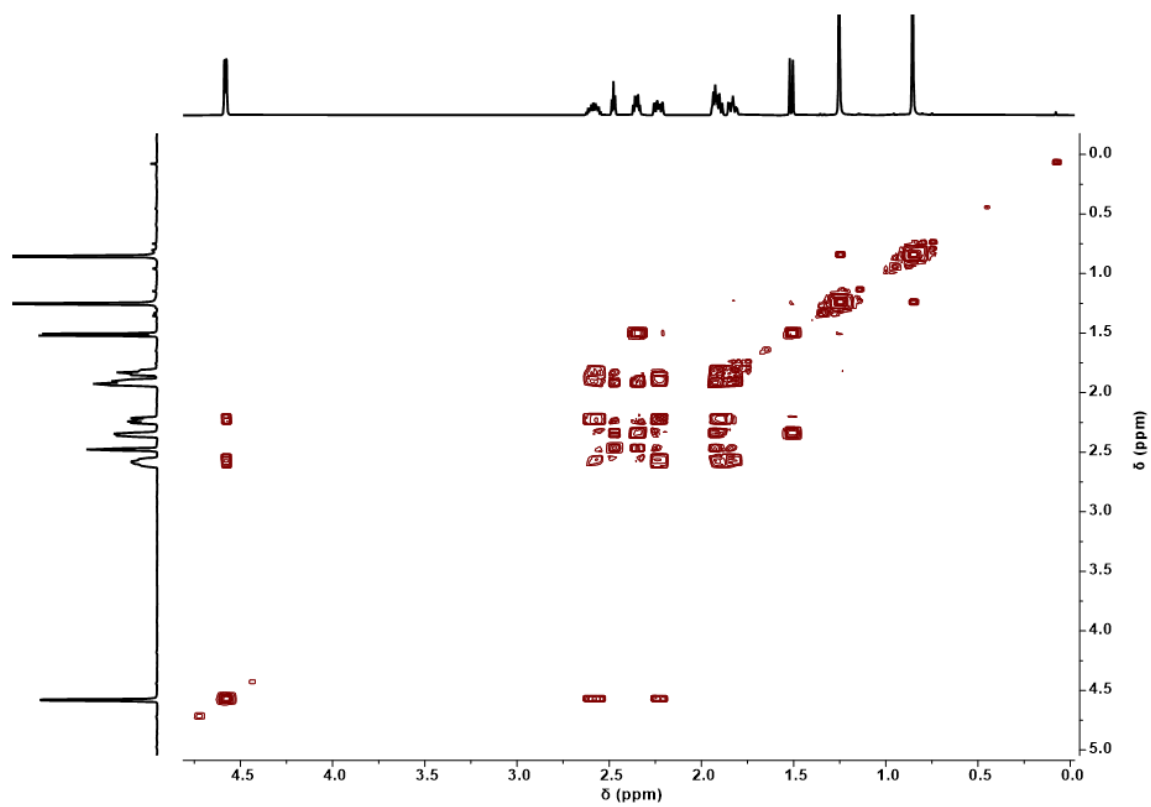
**Figure S17:**  $^1\text{H}$  NMR Spectrum of **2**



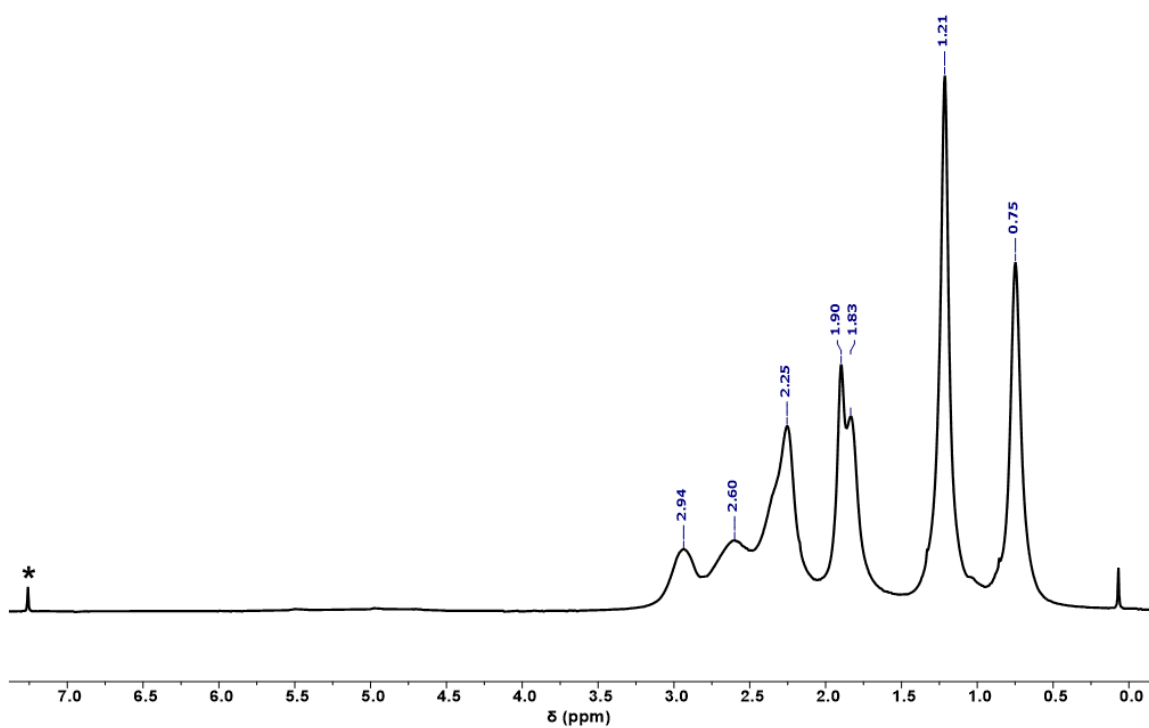
**Figure S18:**  $^{13}\text{C}$  NMR Spectrum of **2**.  $\text{CDCl}_3$  Resonance Represented by \*



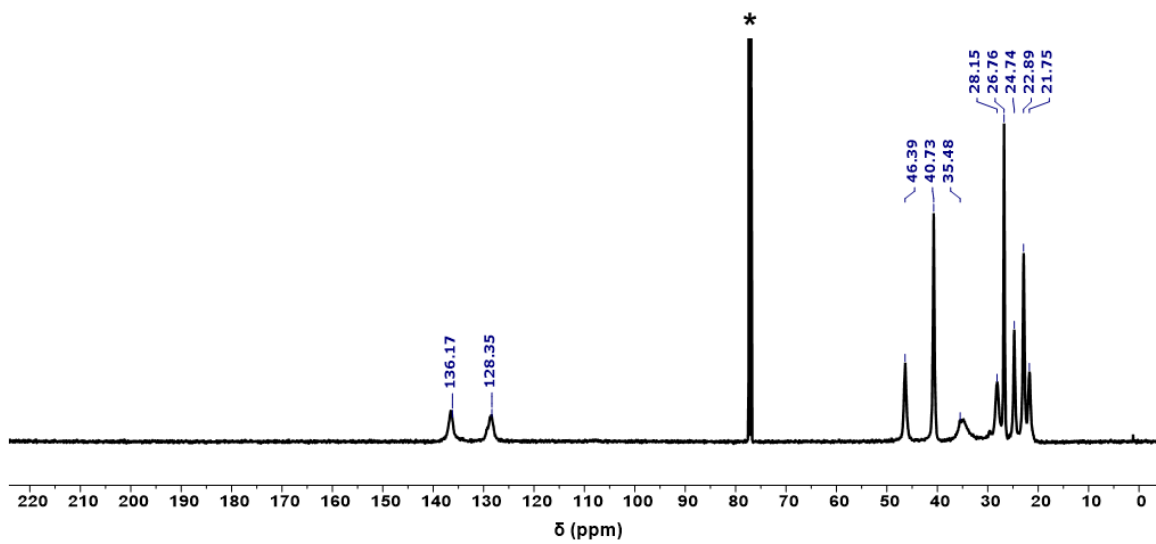
**Figure S19:**  $^1\text{H}$ - $^{13}\text{C}$  HSQC NMR Spectrum of **2**



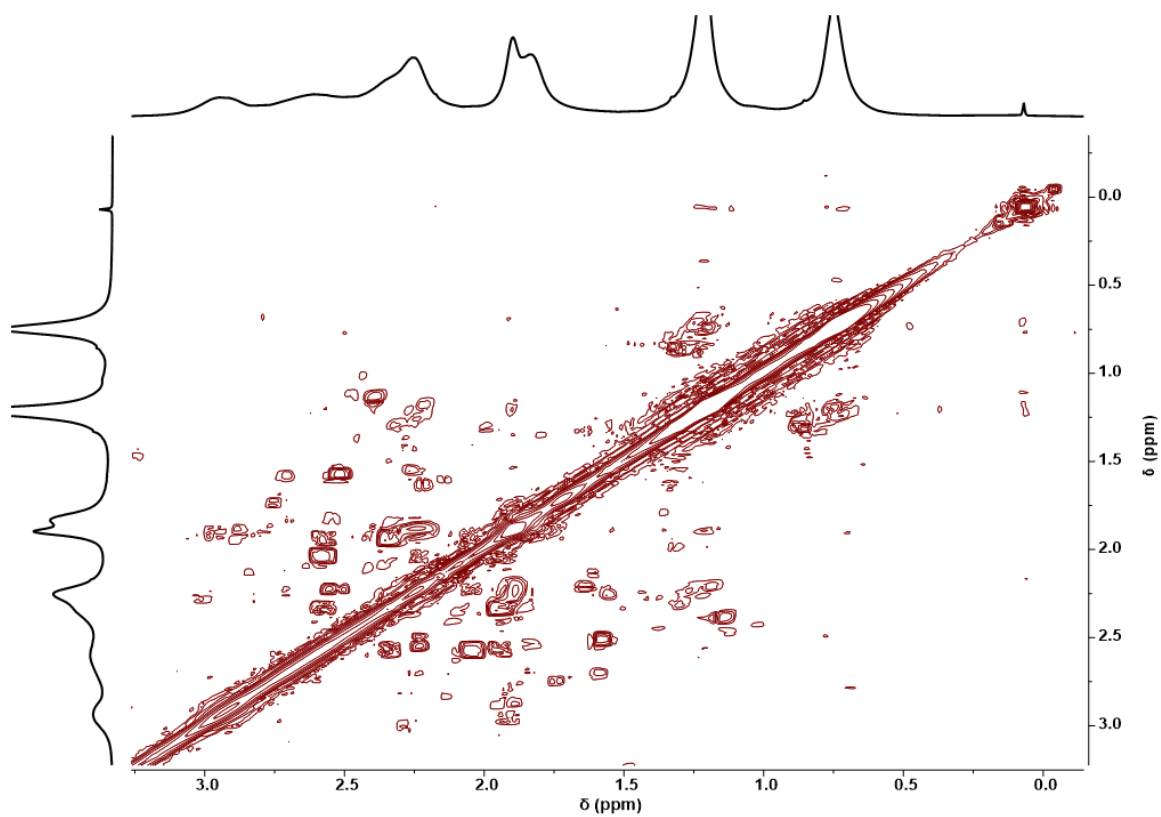
**Figure S20:**  $^1\text{H}$ - $^1\text{H}$  COSY NMR Spectrum of **2**



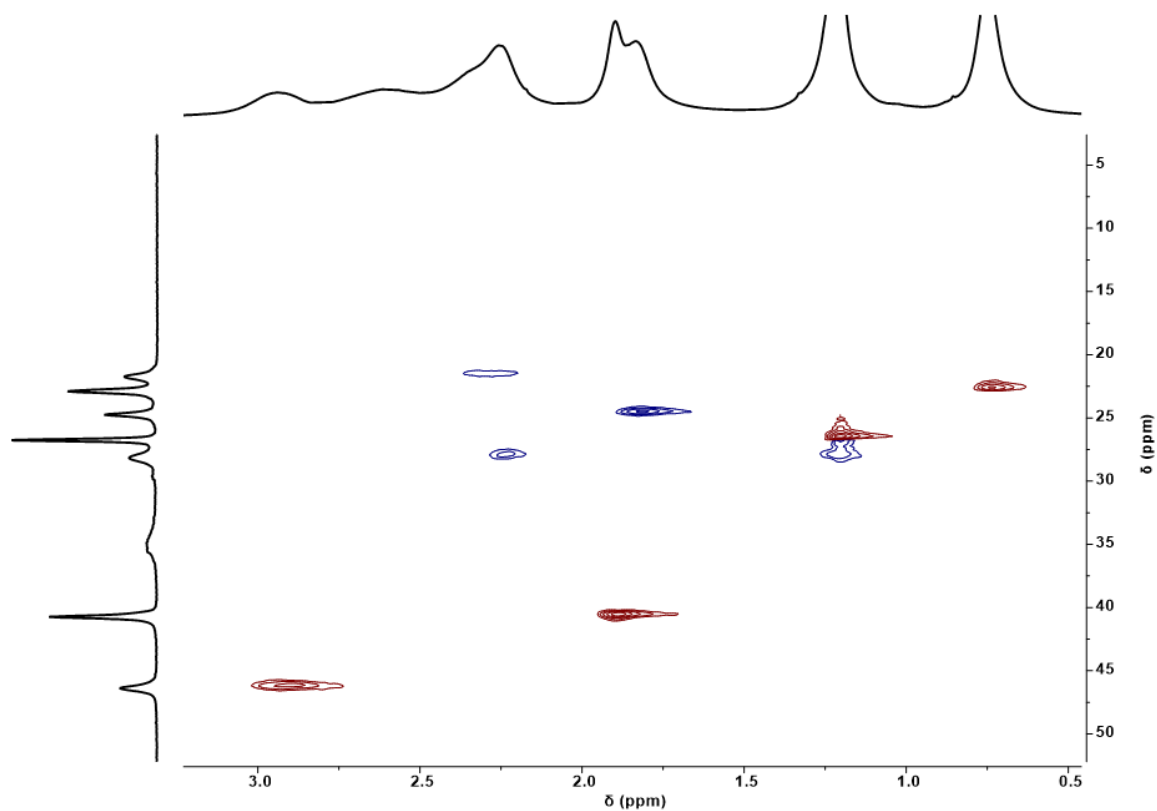
**Figure S21:**  $^1\text{H}$  NMR Spectrum of **3**. Residual  $\text{CHCl}_3$  Represented by \*



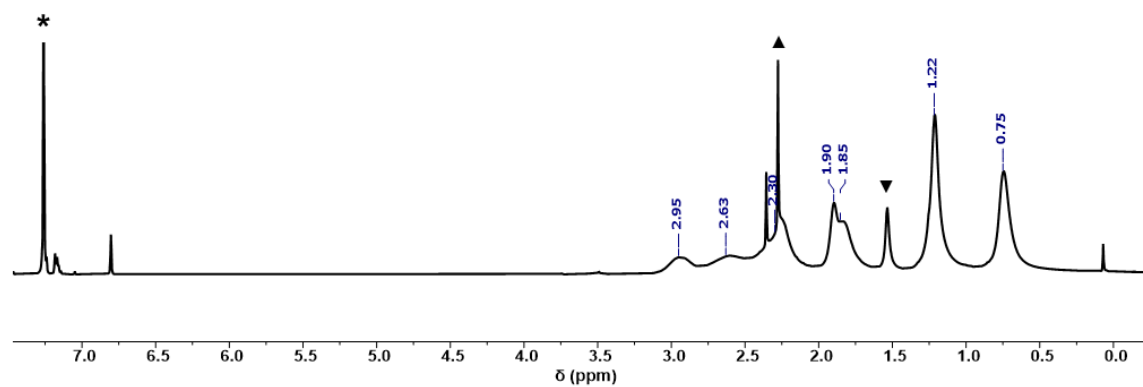
**Figure S22:**  $^{13}\text{C}$  NMR Spectrum of **3**.  $\text{CDCl}_3$  Resonance Represented by \*



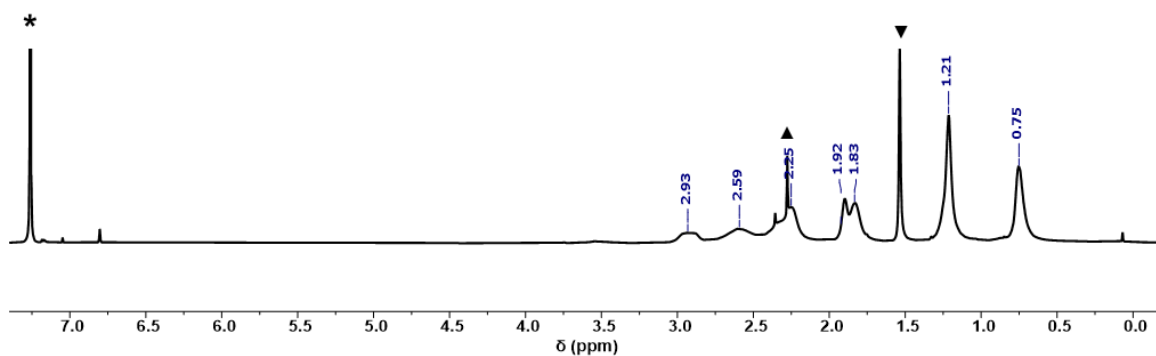
**Figure S23:**  $^1\text{H}$ - $^1\text{H}$  COSY NMR Spectrum of **3**



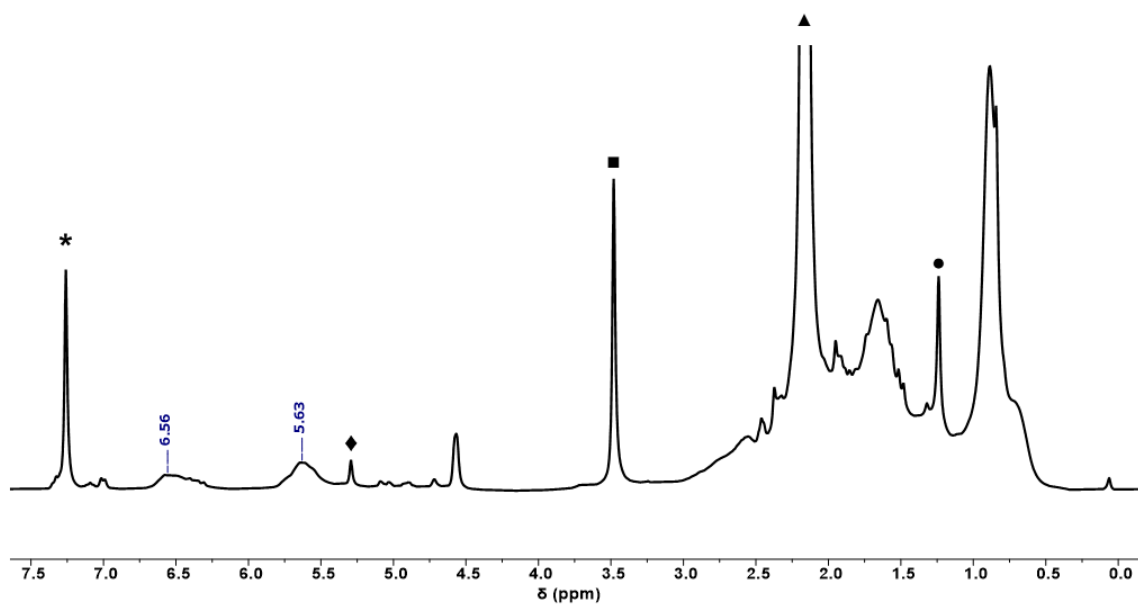
**Figure S24:**  $^1\text{H}$ - $^{13}\text{C}$  HSQC NMR Spectrum of **3**



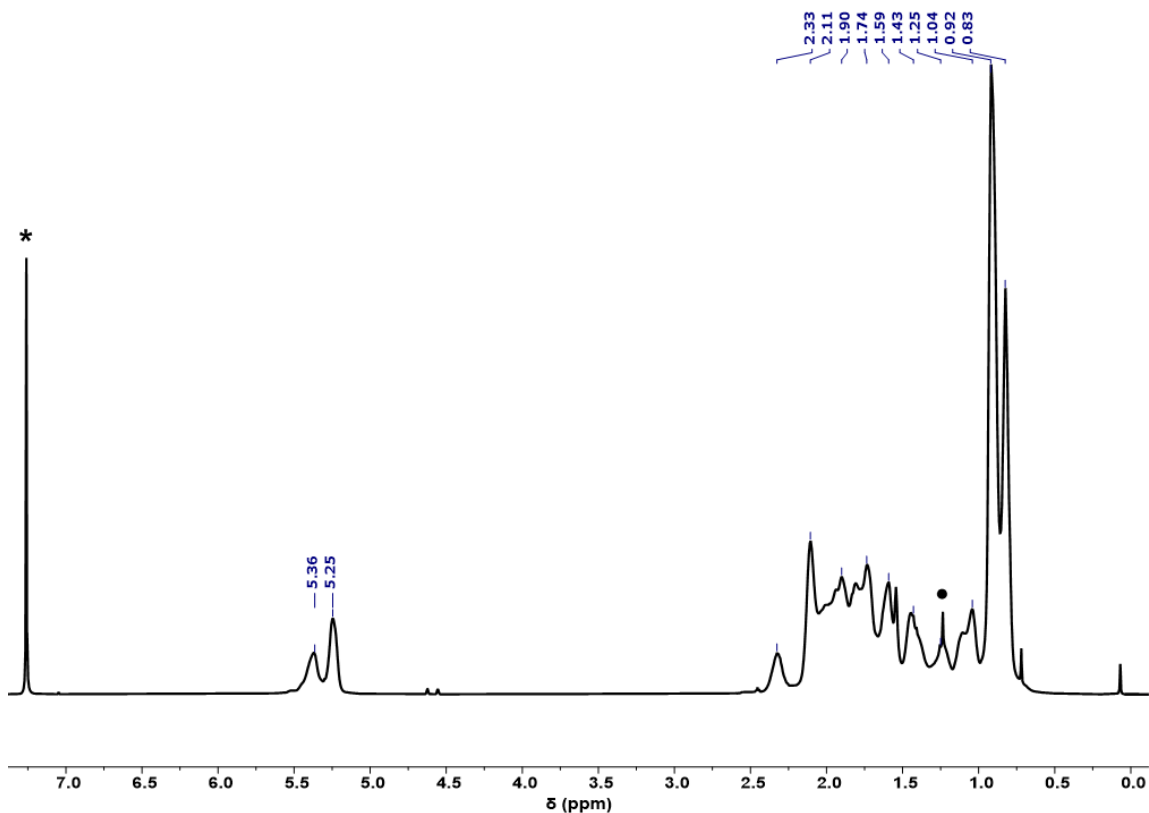
**Figure S25:**  $^1\text{H}$  NMR Spectrum of **2** Polymerized with **5**. Residual  $\text{CHCl}_3$ , Acetone, and Water Represented by \*, ▲, and ▼ Respectively



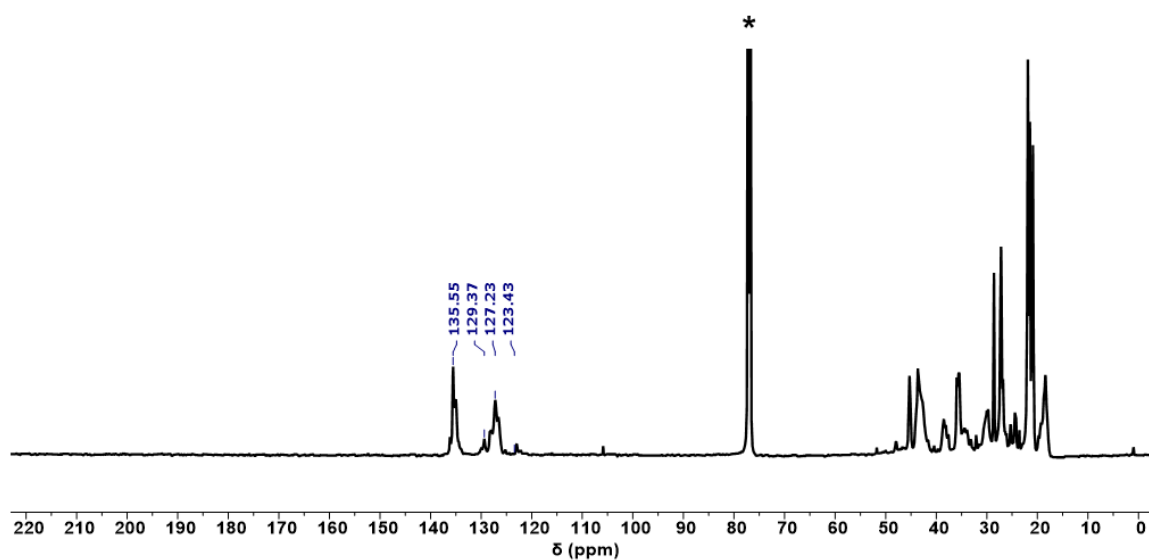
**Figure S26:**  $^1\text{H}$  NMR Spectrum of **2** Polymerized with **6**. Residual  $\text{CHCl}_3$ , Acetone, and Water Represented by \*, ▲, and ▼ Respectively



**Figure S27:**  $^1\text{H}$  NMR Spectrum of the Cationic Ring-Opening Polymerization of **2**.  $\text{CHCl}_3$ , DCM, Methanol, Acetone, and  $\text{Et}_2\text{O}$  represented by \*, ♦, ■, ▲, and ●, respectively

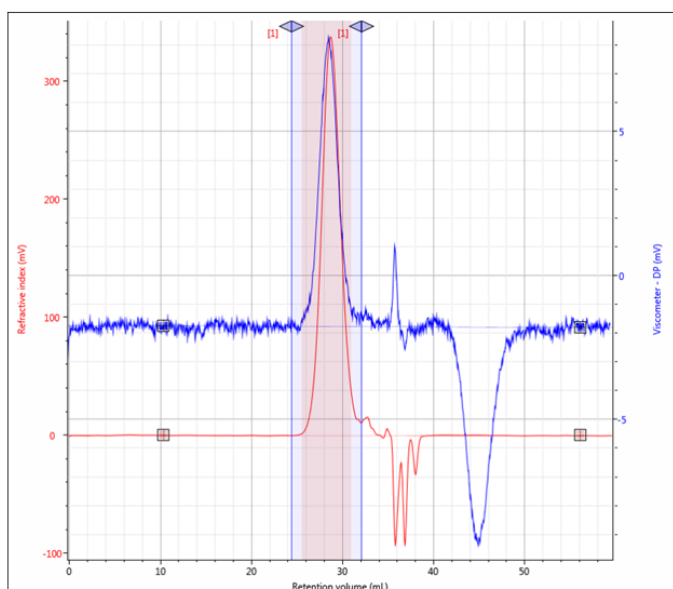


**Figure S28:**  $^1\text{H}$  NMR Spectrum of **7**. Residual  $\text{CHCl}_3$  and  $\text{Et}_2\text{O}$  Represented by \* and •, Respectively



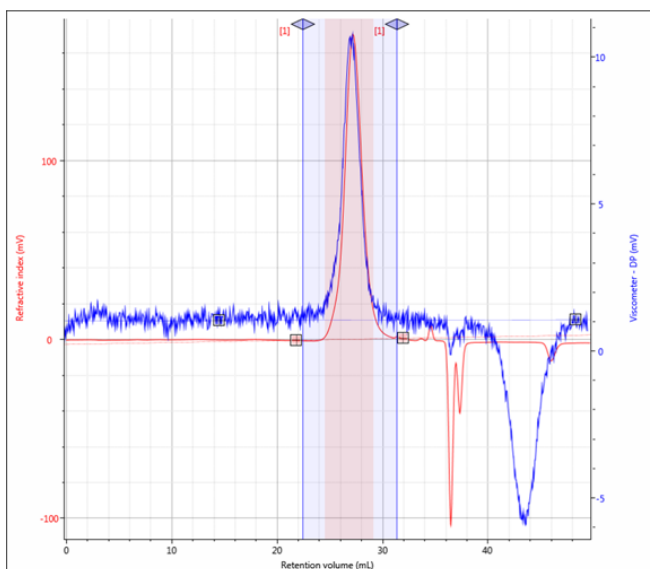
**Figure S29:**  $^{13}\text{C}$  NMR Spectrum of **7**.  $\text{CDCl}_3$  Resonance Represented by \*

## 6 Raw GPC Data



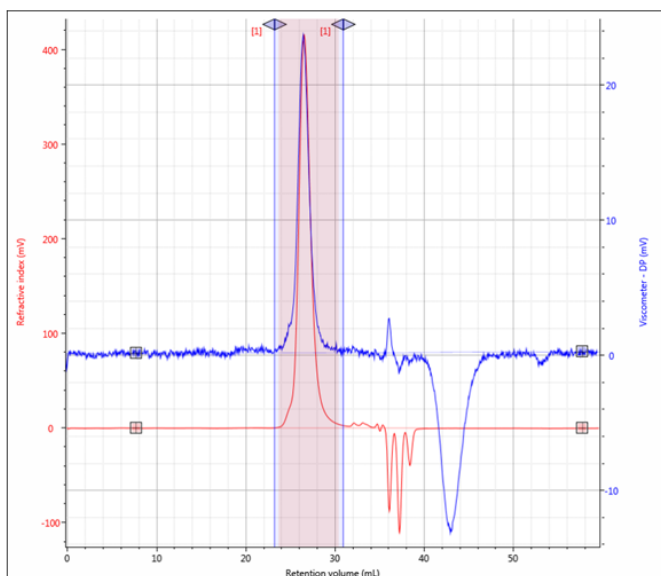
RV (mL) 28.72  
 Mn (g/mol) 7,504  
 Mw (g/mol) 10,290  
 Mz (g/mol) 13,420  
 Mw/Mn 1.371  
 IVw (dL/g) 0.05437  
 Rh( $\eta$ )w (nm) 2.021  
 Rgw (nm) N/C  
 M-H a 0.4446  
 M-H log K (dL/g) -3.034  
 RI peak (mV·mL) 830.6  
 RALS peak (mV·mL) 26.55  
 LALS peak (mV·mL) 19.13  
 DP peak (mV·mL) 24.3  
 MALS peak (mV·mL) N/C  
 Calc. dn/dc 0.1431  
 Recovery (%) N/C

Figure S30: Raw GPC Data for Table S1 Entry 1



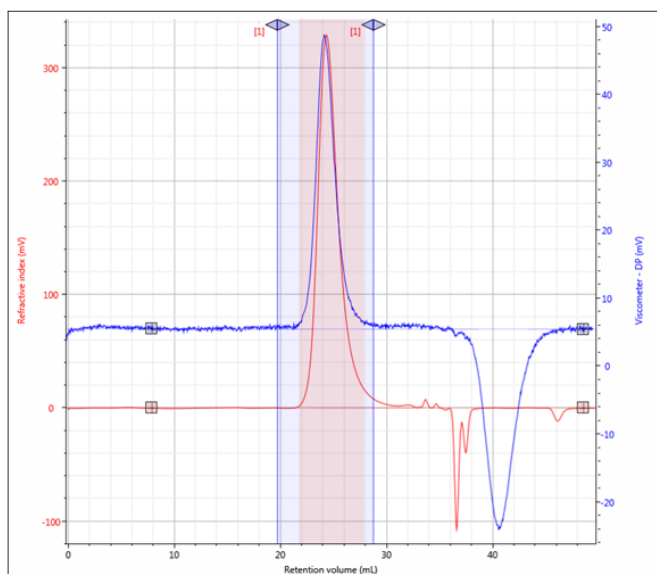
RV (mL) 27.22  
 Mn (g/mol) 18,920  
 Mw (g/mol) 22,540  
 Mz (g/mol) 45,450  
 Mw/Mn 1.192  
 IVw (dL/g) 0.06982  
 Rh( $\eta$ )w (nm) 2.843  
 Rgw (nm) N/C  
 M-H a 0.686  
 M-H log K (dL/g) -4.13  
 RI peak (mV·mL) 340.2  
 RALS peak (mV·mL) 17.72  
 LALS peak (mV·mL) 14  
 DP peak (mV·mL) 20.51  
 MALS peak (mV·mL) N/C  
 Calc. dn/dc 0.1137  
 Recovery (%) N/C

Figure S31: Raw GPC Data for Table S1 Entry 2



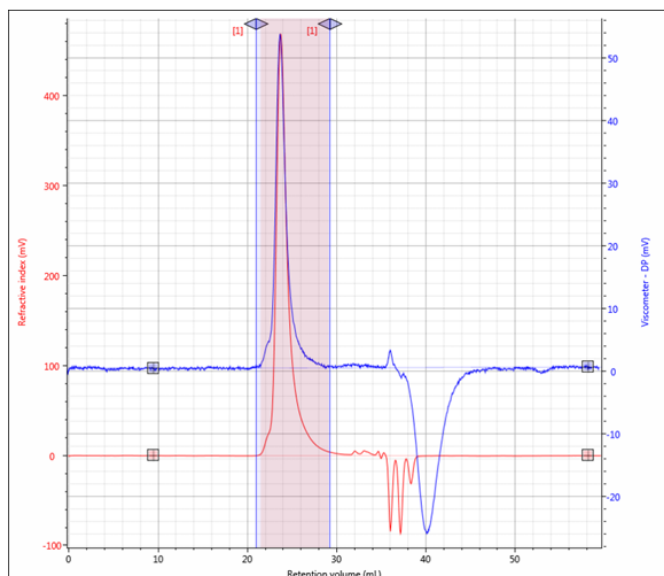
RV (mL) 26.56  
 Mn (g/mol) 26,420  
 Mw (g/mol) 29,720  
 Mz (g/mol) 33,750  
 Mw/Mn 1.125  
 IVw (dL/g) 0.1055  
 Rh( $\eta$ )w (nm) 3.625  
 Rgw (nm) N/C  
 M-H a 0.652  
 M-H log K (dL/g) -3.888  
 RI peak (mV·mL) 674.6  
 RALS peak (mV·mL) 62.56  
 LALS peak (mV·mL) 45.57  
 DP peak (mV·mL) 37.58  
 MALS peak (mV·mL) N/C  
 Calc. dn/dc 0.1437  
 Recovery (%) N/C

**Figure S32:** Raw GPC Data for Table S1 Entry 3



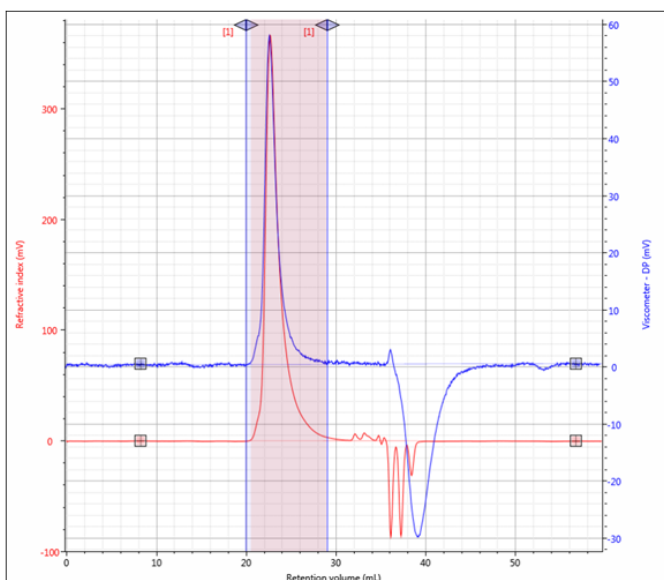
RV (mL) 24.37  
 Mn (g/mol) 52,030  
 Mw (g/mol) 64,050  
 Mz (g/mol) 78,070  
 Mw/Mn 1.231  
 IVw (dL/g) 0.1352  
 Rh( $\eta$ )w (nm) 5.069  
 Rgw (nm) N/C  
 M-H a 0.6352  
 M-H log K (dL/g) -3.912  
 RI peak (mV·mL) 767.6  
 RALS peak (mV·mL) 112.2  
 LALS peak (mV·mL) 86.02  
 DP peak (mV·mL) 95.43  
 MALS peak (mV·mL) N/C  
 Calc. dn/dc 0.1152  
 Recovery (%) N/C

**Figure S33:** Raw GPC Data for Table S1 Entry 4



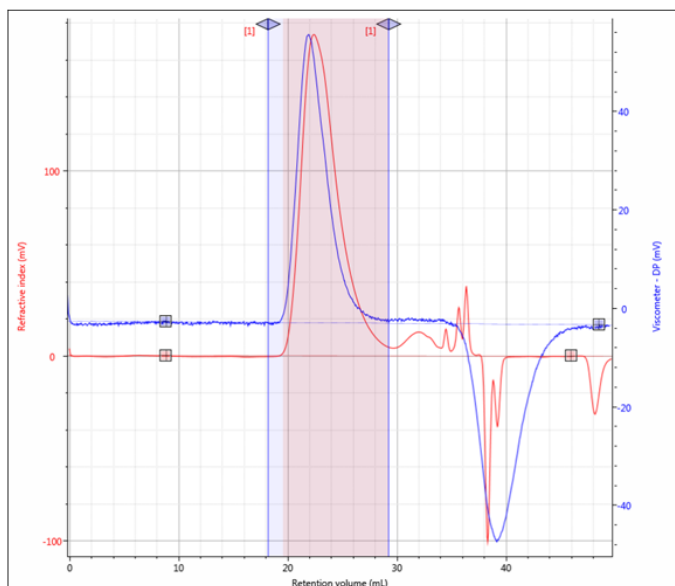
RV (mL) 23.77  
 Mn (g/mol) 66,270  
 Mw (g/mol) 81,440  
 Mz (g/mol) 95,160  
 Mw/Mn 1.229  
 IVw (dL/g) 0.2254  
 Rh( $\eta$ )w (nm) 6.526  
 Rgw (nm) N/C  
 M-H a 0.5149  
 M-H log K (dL/g) -3.17  
 RI peak (mV·mL) 743.2  
 RALS peak (mV·mL) 208.1  
 LALS peak (mV·mL) 152.8  
 DP peak (mV·mL) 80.24  
 MALS peak (mV·mL) N/C  
 Calc. dn/dc 0.1583  
 Recovery (%) N/C

**Figure S34:** Raw GPC Data for Table S1 Entry 5



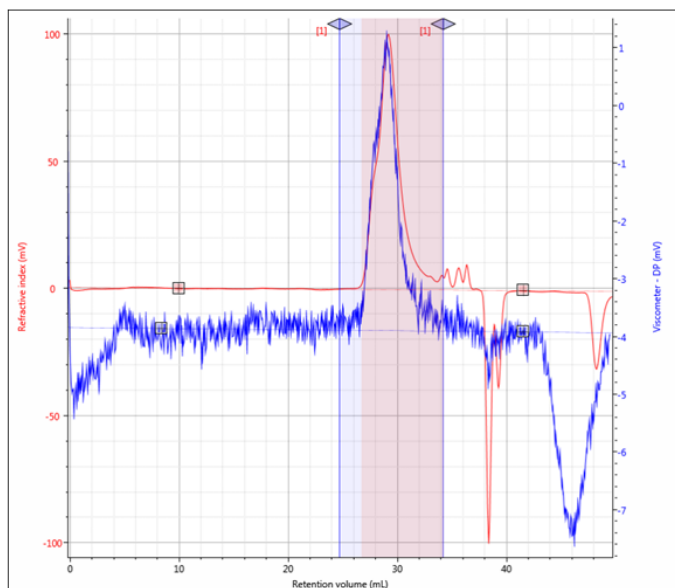
RV (mL) 22.7  
 Mn (g/mol) 99,580  
 Mw (g/mol) 130,200  
 Mz (g/mol) 158,300  
 Mw/Mn 1.308  
 IVw (dL/g) 0.2885  
 Rh( $\eta$ )w (nm) 8.252  
 Rgw (nm) N/C  
 M-H a 0.5731  
 M-H log K (dL/g) -3.465  
 RI peak (mV·mL) 695.3  
 RALS peak (mV·mL) 307.8  
 LALS peak (mV·mL) 227.1  
 DP peak (mV·mL) 97.68  
 MALS peak (mV·mL) N/C  
 Calc. dn/dc 0.1566  
 Recovery (%) N/C

**Figure S35:** Raw GPC Data for Table S1 Entry 6



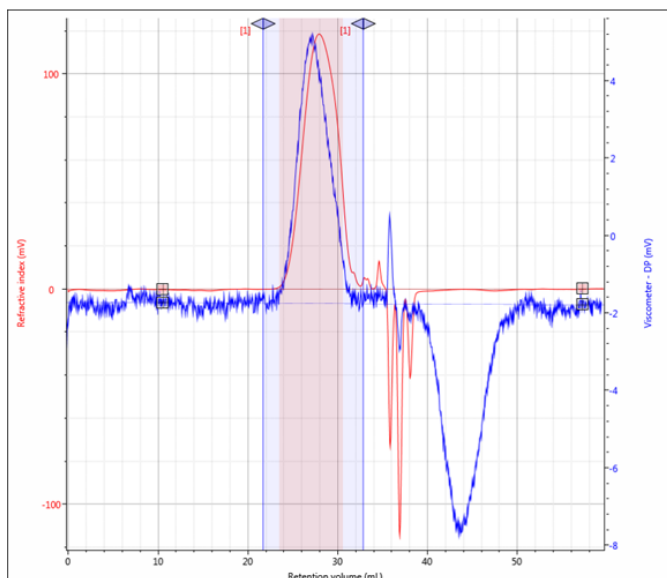
RV (mL) 22.41  
 Mn (g/mol) 159,300  
 Mw (g/mol) 271,000  
 Mz (g/mol) 416,500  
 Mw/Mn 1.701  
 IVw (dL/g) 0.2866  
 Rh( $\eta$ )w (nm) 10.28  
 Rgw (nm) 7.607  
 M-H a 0.6363  
 M-H log K (dL/g) -3.977  
 RI peak (mV·mL) 674.8  
 RALS peak (mV·mL) 371.6  
 LALS peak (mV·mL) 290.9  
 DP peak (mV·mL) 185.5  
 MALS peak (mV·mL) N/C  
 Calc. dn/dc 0.1052  
 Recovery (%) N/C

**Figure S36:** Raw GPC Data for the Vinyl-Addition Polymerization of **2** With **5**



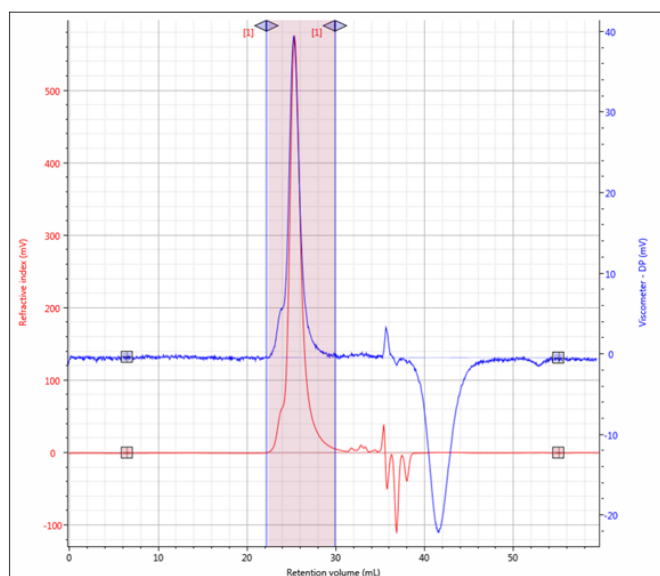
RV (mL) 29.2  
 Mn (g/mol) 15,490  
 Mw (g/mol) 19,510  
 Mz (g/mol) 34,020  
 Mw/Mn 1.26  
 IVw (dL/g) 0.06348  
 Rh( $\eta$ )w (nm) 2.51  
 Rgw (nm) N/C  
 M-H a 0.6582  
 M-H log K (dL/g) -3.983  
 RI peak (mV·mL) 249.4  
 RALS peak (mV·mL) 12.24  
 LALS peak (mV·mL) 10.05  
 DP peak (mV·mL) 13.48  
 MALS peak (mV·mL) N/C  
 Calc. dn/dc 0.1231  
 Recovery (%) N/C

**Figure S37:** Raw GPC Data for the Vinyl-Addition Polymerization of **2** With **6**



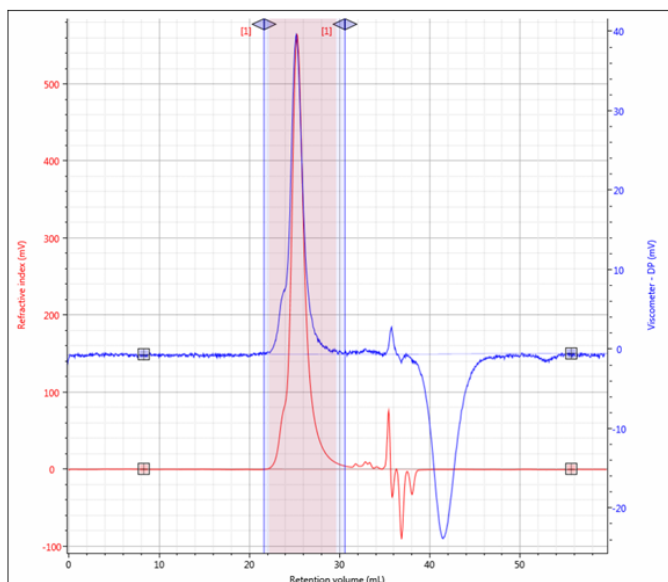
RV (mL) 27.97  
 Mn (g/mol) 5,812  
 Mw (g/mol) 11,110  
 Mz (g/mol) 19,400  
 Mw/Mn 1.912  
 IVw (dL/g) 0.09343  
 Rh(η)w (nm) 2.417  
 Rgw (nm) N/C  
 M-H a 0.5315  
 M-H log K (dL/g) -3.148  
 RI peak (mV·mL) 524.1  
 RALS peak (mV·mL) 16.93  
 LALS peak (mV·mL) 12.13  
 DP peak (mV·mL) 28.14  
 MALS peak (mV·mL) N/C  
 Calc. dn/dc 0.1335  
 Recovery (%) N/C

**Figure S38:** Raw GPC Data for the Cationic Ring-Opening Polymerization of (1S)-(-)-β-pinene



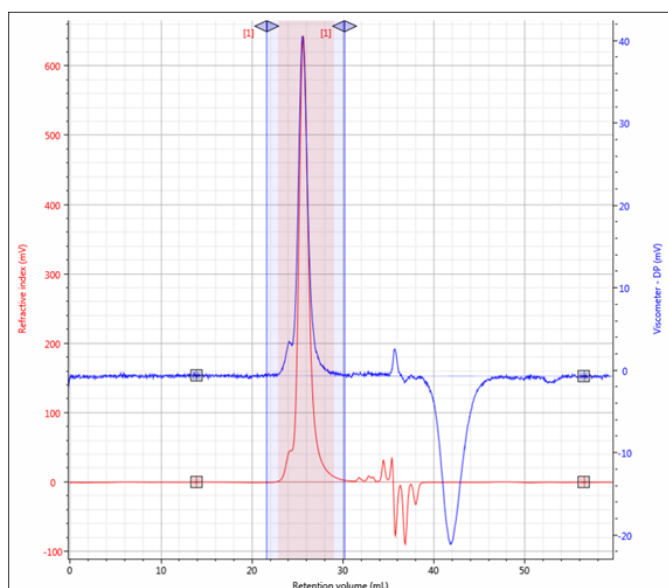
RV (mL) 25.39  
 Mn (g/mol) 39,210  
 Mw (g/mol) 45,530  
 Mz (g/mol) 53,710  
 Mw/Mn 1.161  
 IVw (dL/g) 0.129  
 Rh(η)w (nm) 4.46  
 Rgw (nm) N/C  
 M-H a 0.5725  
 M-H log K (dL/g) -3.549  
 RI peak (mV·mL) 939.1  
 RALS peak (mV·mL) 131.3  
 LALS peak (mV·mL) 95.92  
 DP peak (mV·mL) 63.82  
 MALS peak (mV·mL) N/C  
 Calc. dn/dc 0.1428  
 Recovery (%) N/C

**Figure S39:** Raw GPC Data for the Polymerization of 2 With 4 in Toluene (for Solvent Screen)



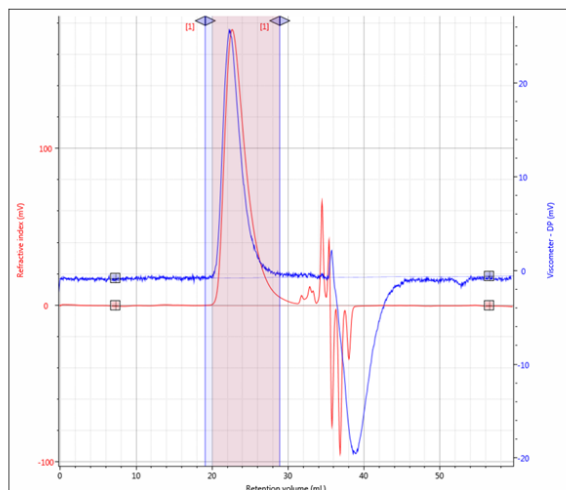
|                    |        |
|--------------------|--------|
| RV (mL)            | 25.32  |
| Mn (g/mol)         | 36,500 |
| Mw (g/mol)         | 46,450 |
| Mz (g/mol)         | 56,760 |
| Mw/Mn              | 1.272  |
| IVw (dL/g)         | 0.1338 |
| Rh( $\eta$ )w (nm) | 4.539  |
| Rgw (nm)           | N/C    |
| M-H a              | 0.4978 |
| M-H log K (dL/g)   | -3.187 |
| RI peak (mV·mL)    | 1,037  |
| RALS peak (mV·mL)  | 149.5  |
| LALS peak (mV·mL)  | 109.4  |
| DP peak (mV·mL)    | 72.42  |
| MALS peak (mV·mL)  | N/C    |
| Calc. dn/dc        | 0.1444 |
| Recovery (%)       | N/C    |

**Figure S40:** Raw GPC Data for the Polymerization of **2** With **4** in Toluene at 35 °C (for Solvent Screen)



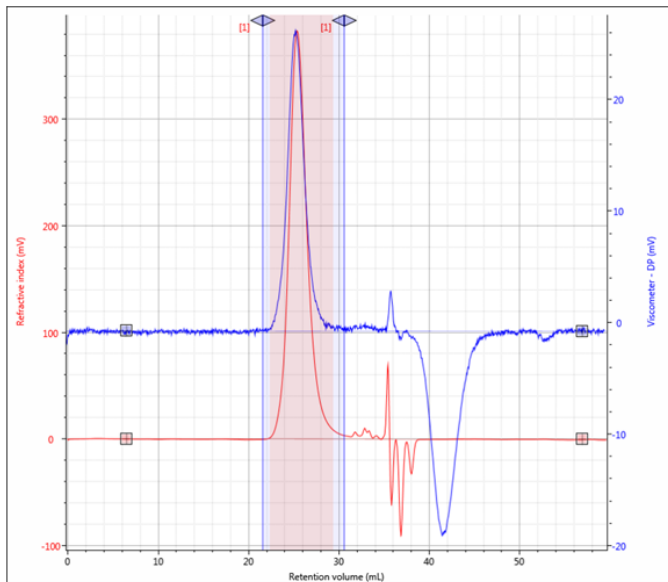
|                    |        |
|--------------------|--------|
| RV (mL)            | 25.67  |
| Mn (g/mol)         | 33,840 |
| Mw (g/mol)         | 39,300 |
| Mz (g/mol)         | 45,390 |
| Mw/Mn              | 1.161  |
| IVw (dL/g)         | 0.1234 |
| Rh( $\eta$ )w (nm) | 4.202  |
| Rgw (nm)           | N/C    |
| M-H a              | 0.5701 |
| M-H log K (dL/g)   | -3.522 |
| RI peak (mV·mL)    | 877.8  |
| RALS peak (mV·mL)  | 107.6  |
| LALS peak (mV·mL)  | 78.52  |
| DP peak (mV·mL)    | 56.19  |
| MALS peak (mV·mL)  | N/C    |
| Calc. dn/dc        | 0.1449 |
| Recovery (%)       | N/C    |

**Figure S41:** Raw GPC Data for the Polymerization of **2** With **4** in Et<sub>2</sub>O (for Solvent Screen)



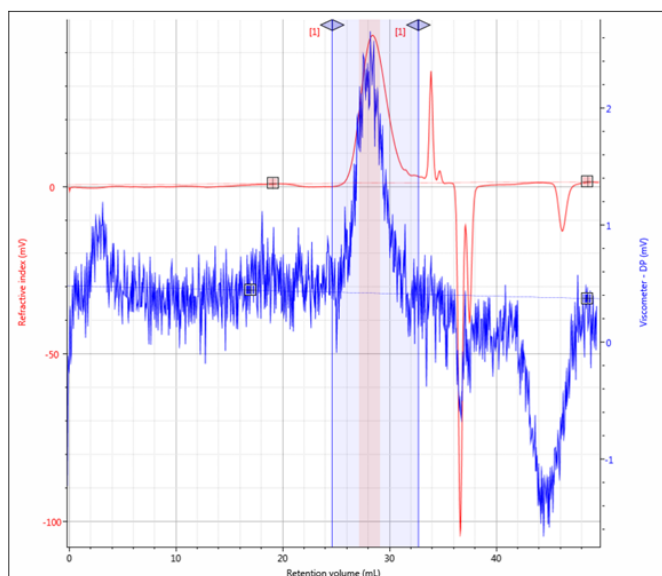
|                    |         |
|--------------------|---------|
| RV (mL)            | 22.68   |
| Mn (g/mol)         | 95,400  |
| Mw (g/mol)         | 148,400 |
| Mz (g/mol)         | 204,800 |
| Mw/Mn              | 1.556   |
| IVw (dL/g)         | 0.2151  |
| Rh( $\eta$ )w (nm) | 7.716   |
| Rgw (nm)           | N/C     |
| M-H a              | 0.5683  |
| M-H log K (dL/g)   | -3.587  |
| RI peak (mV·mL)    | 591     |
| RALS peak (mV·mL)  | 242.3   |
| LALS peak (mV·mL)  | 179.3   |
| DP peak (mV·mL)    | 74.12   |
| MALS peak (mV·mL)  | N/C     |
| Calc. dn/dc        | 0.1289  |
| Recovery (%)       | N/C     |

**Figure S42:** Raw GPC Data for the Polymerization of **2** With **4** in THF (for Solvent Screen)



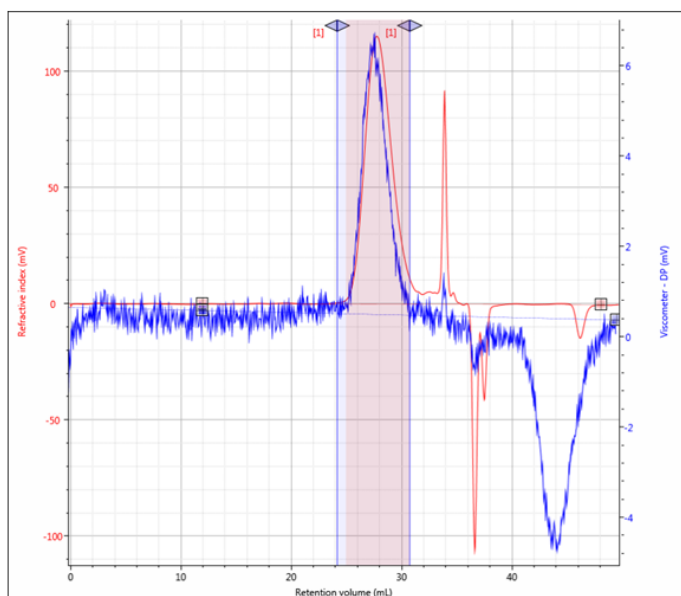
|                    |        |
|--------------------|--------|
| RV (mL)            | 25.41  |
| Mn (g/mol)         | 35,300 |
| Mw (g/mol)         | 45,500 |
| Mz (g/mol)         | 56,650 |
| Mw/Mn              | 1.289  |
| IVw (dL/g)         | 0.1293 |
| Rh( $\eta$ )w (nm) | 4.447  |
| Rgw (nm)           | N/C    |
| M-H a              | 0.5585 |
| M-H log K (dL/g)   | -3.479 |
| RI peak (mV·mL)    | 901.5  |
| RALS peak (mV·mL)  | 125.9  |
| LALS peak (mV·mL)  | 92.21  |
| DP peak (mV·mL)    | 61.47  |
| MALS peak (mV·mL)  | N/C    |
| Calc. dn/dc        | 0.1427 |
| Recovery (%)       | N/C    |

**Figure S43:** Raw GPC Data for the Polymerization of **2** With **4** in DCM (for Solvent Screen)



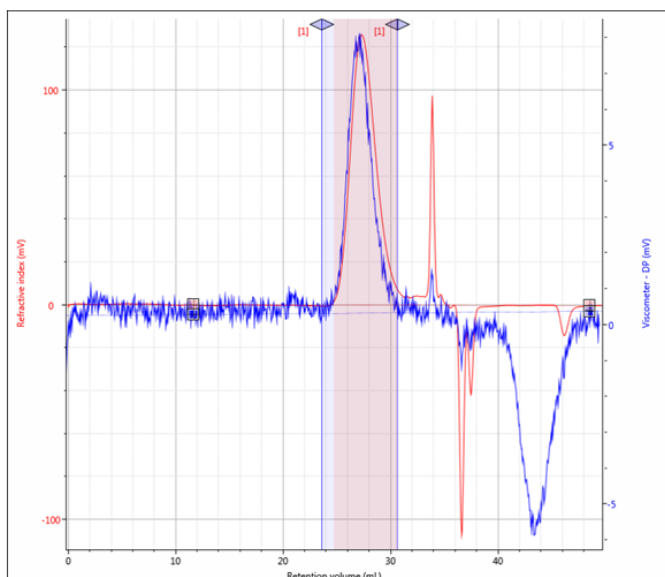
RV (mL) 28.45  
 Mn (g/mol) 8,734  
 Mw (g/mol) 11,090  
 Mz (g/mol) 14,260  
 Mw/Mn 1.27  
 IVw (dL/g) 0.06282  
 Rh( $\eta$ )w (nm) 2.097  
 Rgw (nm) N/C  
 M-H a -1.337  
 M-H log K (dL/g) 4.078  
 RI peak (mV·mL) 127.3  
 RALS peak (mV·mL) 5.028  
 LALS peak (mV·mL) 4.288  
 DP peak (mV·mL) 5.605  
 MALS peak (mV·mL) N/C  
 Calc. dn/dc 0.1372  
 Recovery (%) N/C

**Figure S44:** Raw GPC Data for Table S5 Entry 2



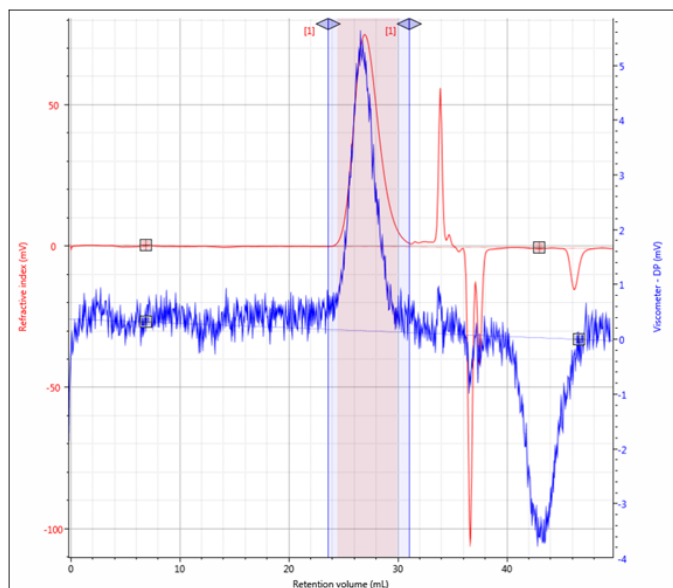
RV (mL) 27.79  
 Mn (g/mol) 13,110  
 Mw (g/mol) 15,750  
 Mz (g/mol) 22,370  
 Mw/Mn 1.202  
 IVw (dL/g) 0.06212  
 Rh( $\eta$ )w (nm) 2.414  
 Rgw (nm) N/C  
 M-H a 0.9581  
 M-H log K (dL/g) -5.167  
 RI peak (mV·mL) 327.9  
 RALS peak (mV·mL) 13.7  
 LALS peak (mV·mL) 10.9  
 DP peak (mV·mL) 16.1  
 MALS peak (mV·mL) N/C  
 Calc. dn/dc 0.134  
 Recovery (%) N/C

**Figure S45:** Raw GPC Data for Table S5 Entry 3



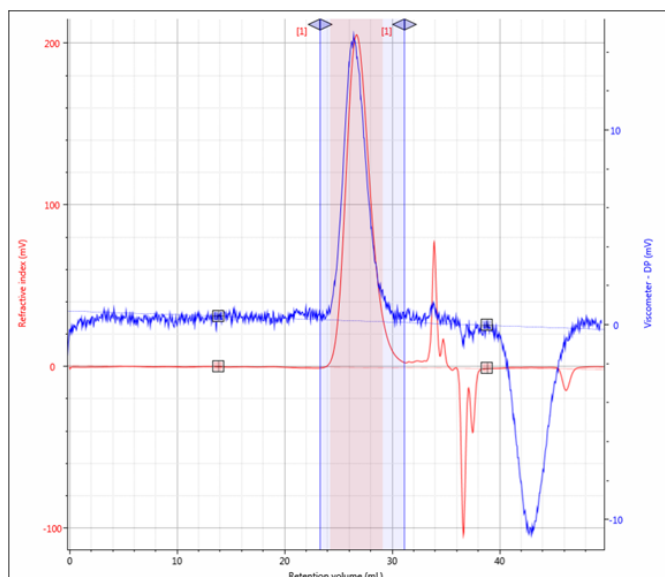
RV (mL) 27.34  
 Mn (g/mol) 15,150  
 Mw (g/mol) 18,140  
 Mz (g/mol) 25,200  
 Mw/Mn 1.197  
 IVw (dL/g) 0.0737  
 Rh( $\eta$ )w (nm) 2.691  
 Rgw (nm) N/C  
 M-H a 0.7635  
 M-H log K (dL/g) -4.386  
 RI peak (mV·mL) 348.5  
 RALS peak (mV·mL) 16.87  
 LALS peak (mV·mL) 13.01  
 DP peak (mV·mL) 20.32  
 MALS peak (mV·mL) N/C  
 Calc. dn/dc 0.1333  
 Recovery (%) N/C

**Figure S46:** Raw GPC Data for Table S5 Entry 4



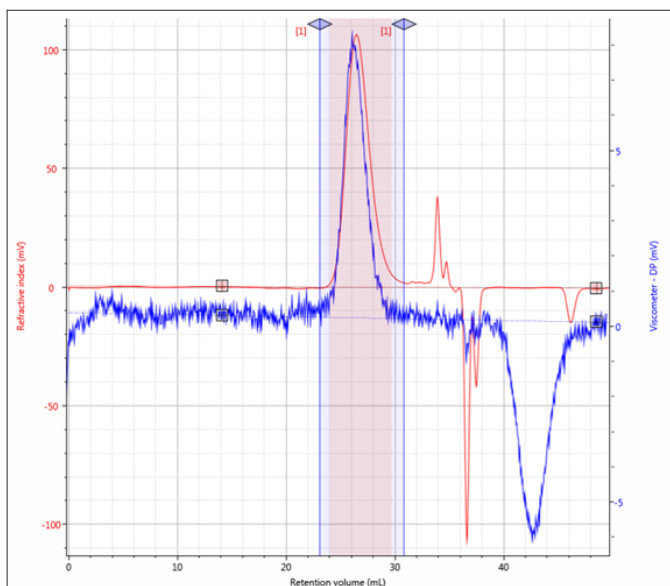
RV (mL) 26.99  
 Mn (g/mol) 16,160  
 Mw (g/mol) 19,540  
 Mz (g/mol) 25,210  
 Mw/Mn 1.209  
 IVw (dL/g) 0.0854  
 Rh( $\eta$ )w (nm) 2.892  
 Rgw (nm) N/C  
 M-H a 0.6796  
 M-H log K (dL/g) -3.973  
 RI peak (mV·mL) 205  
 RALS peak (mV·mL) 10.81  
 LALS peak (mV·mL) 8.287  
 DP peak (mV·mL) 14.25  
 MALS peak (mV·mL) N/C  
 Calc. dn/dc 0.135  
 Recovery (%) N/C

**Figure S47:** Raw GPC Data for Table S5 Entry 5



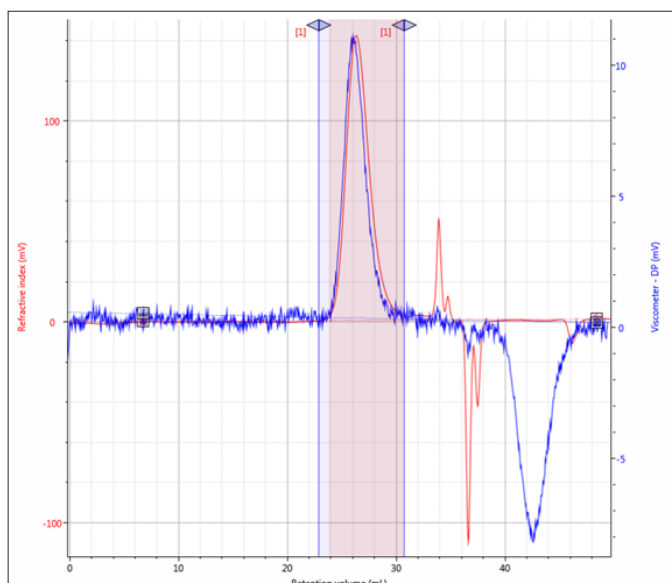
RV (mL) 26.72  
 Mn (g/mol) 17,260  
 Mw (g/mol) 21,240  
 Mz (g/mol) 27,560  
 Mw/Mn 1.231  
 IVw (dL/g) 0.08682  
 Rh( $\eta$ )w (nm) 3.016  
 Rgw (nm) N/C  
 M-H a 0.7006  
 M-H log K (dL/g) -4.08  
 RI peak (mV·mL) 544.6  
 RALS peak (mV·mL) 31.97  
 LALS peak (mV·mL) 25.07  
 DP peak (mV·mL) 36.88  
 MALS peak (mV·mL) N/C  
 Calc. dn/dc 0.1373  
 Recovery (%) N/C

**Figure S48:** Raw GPC Data for Table S5 Entry 6



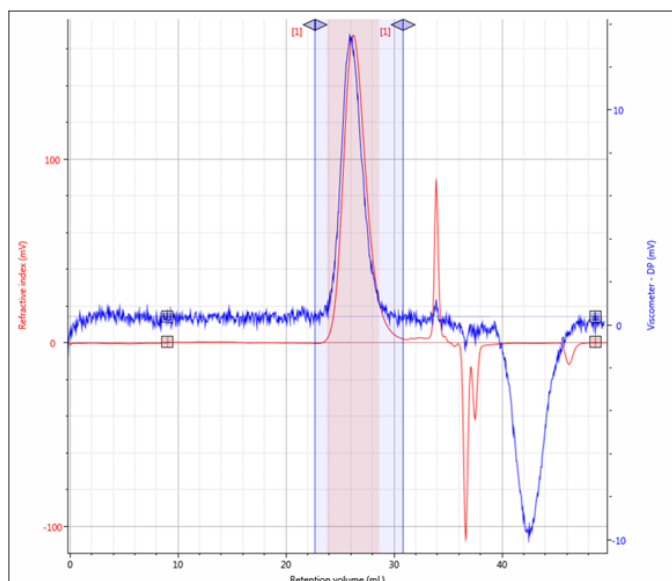
RV (mL) 26.49  
 Mn (g/mol) 20,060  
 Mw (g/mol) 24,060  
 Mz (g/mol) 30,490  
 Mw/Mn 1.199  
 IVw (dL/g) 0.08775  
 Rh( $\eta$ )w (nm) 3.14  
 Rgw (nm) N/C  
 M-H a 0.6954  
 M-H log K (dL/g) -4.093  
 RI peak (mV·mL) 274.1  
 RALS peak (mV·mL) 17.41  
 LALS peak (mV·mL) 13.56  
 DP peak (mV·mL) 19.43  
 MALS peak (mV·mL) N/C  
 Calc. dn/dc 0.1326  
 Recovery (%) N/C

**Figure S49:** Raw GPC Data for Table S5 Entry 7



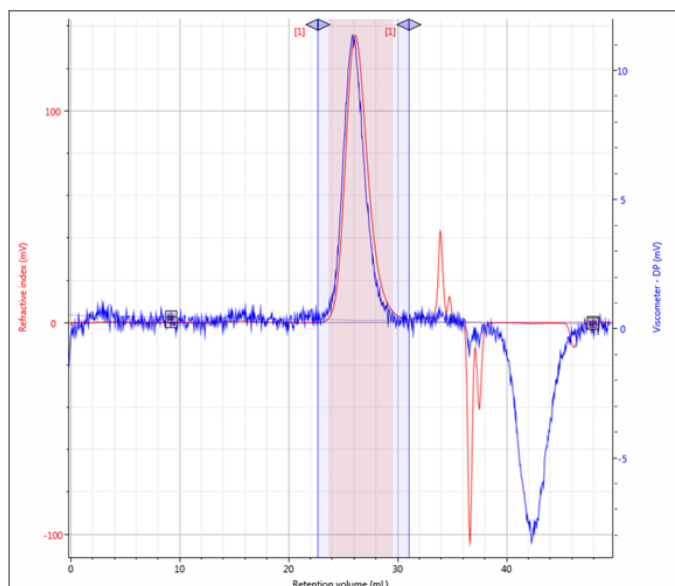
RV (mL) 26.36  
 Mn (g/mol) 20,690  
 Mw (g/mol) 24,760  
 Mz (g/mol) 31,150  
 Mw/Mn 1.197  
 IVw (dL/g) 0.09111  
 Rh( $\eta$ )w (nm) 3.213  
 Rgw (nm) N/C  
 M-H a 0.7518  
 M-H log K (dL/g) -4.331  
 RI peak (mV·mL) 359.4  
 RALS peak (mV·mL) 24.22  
 LALS peak (mV·mL) 18.75  
 DP peak (mV·mL) 25.15  
 MALS peak (mV·mL) N/C  
 Calc. dn/dc 0.1374  
 Recovery (%) N/C

**Figure S50:** Raw GPC Data for Table S5 Entry 8



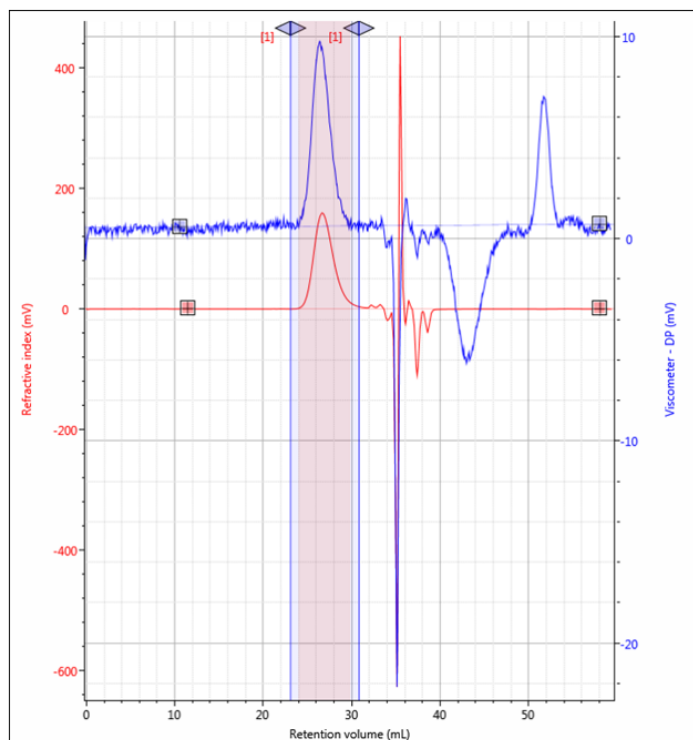
RV (mL) 26.26  
 Mn (g/mol) 22,120  
 Mw (g/mol) 26,870  
 Mz (g/mol) 35,200  
 Mw/Mn 1.215  
 IVw (dL/g) 0.0912  
 Rh( $\eta$ )w (nm) 3.317  
 Rgw (nm) N/C  
 M-H a 0.9472  
 M-H log K (dL/g) -5.247  
 RI peak (mV·mL) 416.9  
 RALS peak (mV·mL) 29.62  
 LALS peak (mV·mL) 23.16  
 DP peak (mV·mL) 29.91  
 MALS peak (mV·mL) N/C  
 Calc. dn/dc 0.1318  
 Recovery (%) N/C

**Figure S51:** Raw GPC Data for Table S5 Entry 9



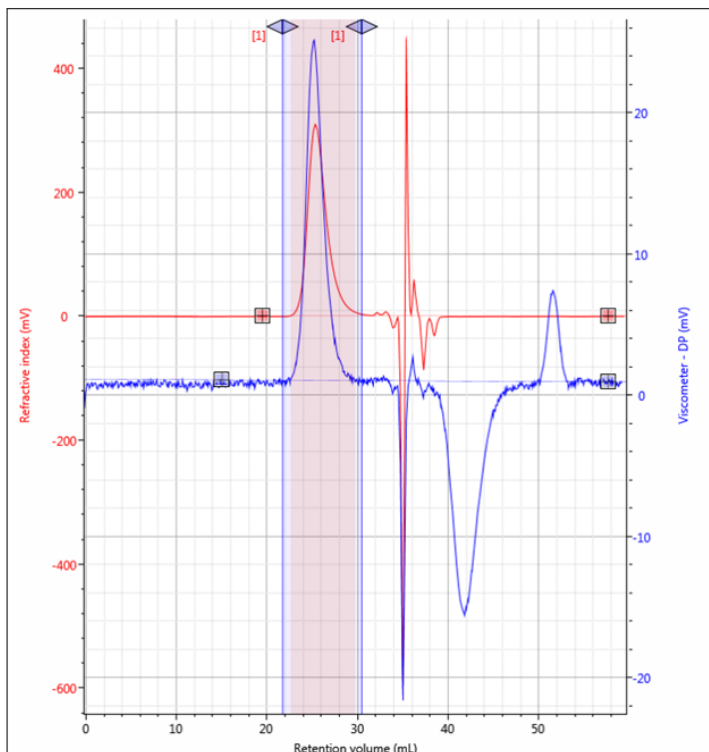
RV (mL) 26.14  
 Mn (g/mol) 23,170  
 Mw (g/mol) 27,780  
 Mz (g/mol) 34,740  
 Mw/Mn 1.199  
 IVw (dL/g) 0.09502  
 Rh( $\eta$ )w (nm) 3.392  
 Rgw (nm) N/C  
 M-H a 0.7161  
 M-H log K (dL/g) -4.186  
 RI peak (mV·mL) 333.9  
 RALS peak (mV·mL) 24.34  
 LALS peak (mV·mL) 18.76  
 DP peak (mV·mL) 25.47  
 MALS peak (mV·mL) N/C  
 Calc. dn/dc 0.1319  
 Recovery (%) N/C

**Figure S52:** Raw GPC Data for Table S5 Entry 10



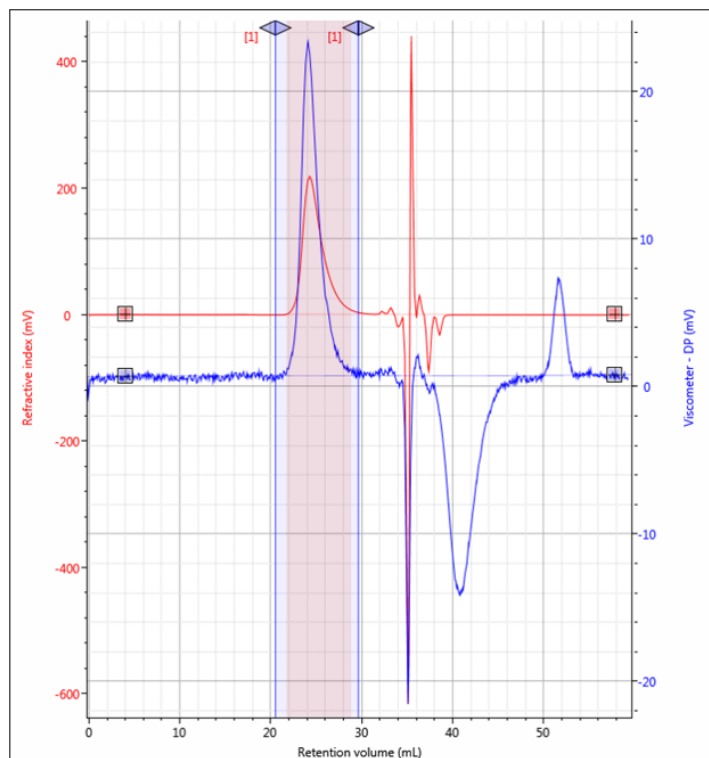
RV (mL) 26.71  
 Mn (g/mol) 28,530  
 Mw (g/mol) 37,210  
 Mz (g/mol) 46,590  
 Mw/Mn 1.304  
 IVw (dL/g) 0.07822  
 Rh( $\eta$ )w (nm) 3.512  
 Rgw (nm) N/C  
 M-H a 0.6233  
 M-H log K (dL/g) -3.952  
 RI peak (mV·mL) 418.9  
 RALS peak (mV·mL) 37.76  
 LALS peak (mV·mL) 27.6  
 DP peak (mV·mL) 22.14  
 MALS peak (mV·mL) N/C  
 Calc. dn/dc 0.1115  
 Recovery (%) N/C

**Figure S53:** Raw GPC Data for Table S6 Entry 1



RV (mL) 25.39  
 Mn (g/mol) 45,420  
 Mw (g/mol) 58,940  
 Mz (g/mol) 72,720  
 Mw/Mn 1.298  
 IVw (dL/g) 0.1085  
 Rh( $\eta$ )w (nm) 4.573  
 Rgw (nm) N/C  
 M-H a 0.6183  
 M-H log K (dL/g) -3.905  
 RI peak (mV·mL) 764.9  
 RALS peak (mV·mL) 113.9  
 LALS peak (mV·mL) 83.22  
 DP peak (mV·mL) 54.47  
 MALS peak (mV·mL) N/C  
 Calc. dn/dc 0.1164  
 Recovery (%) N/C

**Figure S54:** Raw GPC Data for Table S6 Entry 2



RV (mL) 24.32  
 Mn (g/mol) 59,590  
 Mw (g/mol) 81,240  
 Mz (g/mol) 103,700  
 Mw/Mn 1.363  
 IVw (dL/g) 0.1539  
 Rh( $\eta$ )w (nm) 5.699  
 Rgw (nm) N/C  
 M-H a 0.5577  
 M-H log K (dL/g) -3.536  
 RI peak (mV·mL) 566.8  
 RALS peak (mV·mL) 128.9  
 LALS peak (mV·mL) 94.43  
 DP peak (mV·mL) 52.16  
 MALS peak (mV·mL) N/C  
 Calc. dn/dc 0.1289  
 Recovery (%) N/C

**Figure S55:** Raw GPC Data for Table S6 Entry 3

## 7 **References**

- (1) Mühlstädt, M.; Thanh, L. Q.; Graefe, J. *Tetrahedron* **1972**, 28, 4389–4393.
- (2) Nizovtsev, A. V.; Baird, M. S.; Bolesov, I. G. *Tetrahedron* **2004**, 60 (16), 3717–3729.
- (3) Kukhta, N. A.; Vasilenko, I. V.; Kostjuk, S. V. *Green Chem.* **2011**, 13 (9), 2362–2364.
- (4) Satoh, K.; Nakahara, A.; Mukunoki, K.; Sugiyama, H.; Saito, H.; Kamigaito, M. *Polym. Chem.* **2014**, 5, 3222–3230.
- (5) Yu, P.; Li, A.-L.; Liang, H.; Lu, J. *J. Polym. Sci. Part A Polym. Chem.* **2007**, 45, 3739–3746.